This is a preprint, the final version is subject to change, of the American Mineralogist (MSA)
Cite as Authors (Year) Title. American Mineralogist, in press.
DOI: https://doi.org/10.2138/am-2020-7119

**REVISION 1**

# Enigmatic diamonds from the Tolbachik volcano, Kamchatka

Erik M. Galimov[1], Felix V. Kaminsky[1,*], Svetlana N. Shilobreeva[1], Vyacheslav S. Sevastyanov[1], Sergei A. Voropaev[1], Galina K. Khachatryan[2], Richard Wirth[3], Anja Schreiber[3], Vladimir V. Saraykin[4], Gennady A. Karpov[5], Leonid P. Anikin[5]

[1]Vernadsky Institute of Geochemistry and Analytical Chemistry, Russian Academy of Sciences, Kosygin Street 19, Moscow 119334, Russian Federation

[2]Central Research Institute of Geological Prospecting for Base and Precious Metals, Varshavskoye Shosse 129, Moscow 117545, Russian Federation

[3]Helmholtz Centre Potsdam, GFZ German Research Center for Geosciences, 3.5 Surface Geochemistry, Telegrafenberg, C120, D-14473 Potsdam, Germany

[4]Institute of Physical Problems, Zelenograd 124460, Russian Federation

[5]Institute of Volcanology and Seismology, Russian Academy of Sciences, Petropavlovsk–Kamchatskii 683006, Russian Federation

## ABSTRACT

Approximately 700 diamond crystals were identified in volcanic (mainly pyroclastic) rocks of the Tolbachik volcano, Kamchatka, Russia. They were studied with the use of SIMS, scanning and transmission electron microscopy and utilization of electron energy loss spectroscopy and electron diffraction. Diamonds have cube-octahedral shape and extremely homogeneous internal structure. Two groups of impurity elements are distinguished by their distribution within the diamond. First group, N and

*Corresponding author. E-mail: kaminsky@geokhi.ru

H, the most common structural impurities in diamond, are distributed homogeneously. All other elements observed (Cl, F, O, S, Si, Al, Ca, and K) form local concentrations, implying the existence of inclusions, causing high concentrations of these elements. Most elements have concentrations 3-4 orders of magnitude less than chondritic values. Besides N and H, Si, F, Cl, and Na are relatively enriched because they are concentrated in micro- and nanoinclusions in diamond. Mineral inclusions in the studied diamonds are 70-450 nm in size, round- or oval-shaped. They are represented by two mineral groups: Mn-Ni alloys and silicides, with wide range of concentrations for each group. Alloys vary in stoichiometry from MnNi to $Mn_2Ni$, with a minor admixture of Si from 0 to 5.20-5.60 at.%. Silicides, usually coexisting with alloys, vary in composition from $(Mn,Ni)_4Si$ to $(Mn,Ni)_5Si_2$ and $Mn_5Si_2$, and further to MnSi, forming pure Mn-silicides. Mineral inclusions have nanometre-sized bubbles that contain a fluid or a gas phase (F and O). Carbon isotopic compositions in diamonds vary from -21 ‰ to -29 ‰ $\delta^{13}C_{VPDB}$ (av. = -25.4). Nitrogen isotopic compositions in diamond from Tolbachik volcano are from -2.32 ‰ to -2.58 ‰ $\delta^{15}N_{Air}$. Geological, geochemical and mineralogical data confirm the natural origin of studied Tolbachik diamonds from volcanic gases during the explosive stage of the eruption.

**Keywords**: diamond, Kamchatka, cavitation, silicide, carbon isotope, nitrogen isotope, volcanic gases, volatiles

## INTRODUCTION

Numerous finds of diamonds in products of eruption from six volcanoes in Kamchatka and Kuril Islands are known to date. They extend from the Atlasov Island, northern Kuril Islands (the Alaid volcano) in the south up to Koryakia in northern Kamchatka (Kutyev and Kutyeva 1975; Kaminsky et al. 1979, 2016, 2019; Baikov et al. 1995; Seliverstov 2009).

In 2013-2014, a series of diamonds was identified in volcanic rocks of recent (2012-2013) fissure eruption of the Tolbachik volcano (Anikin et al. 2014). They are considered as a phase formed from volcanic fluids (Gordeev et al. 2014; Karpov et al. 2014; Silaev et al. 2015; Galimov et al. 2016a, 2016b).

The existence of diamonds in conditions that do not carry out any evidence of the presence of high pressure in their medium raises discussions about the origin of these diamonds. Suggestions about their origin as the result of cavitation, CVD mechanism, and even that they are the result of technical contamination were expressed. Therefore, we performed an additional, more detailed study of the Tolbachik diamonds that may enlighten the origin of these enigmatic diamonds.

## SAMPLES AND METHODS

### Geological setting

The Plosky (Flat) Tolbachik volcano, 3085 m high, is located at 55º50.0′ N and 160º22.5′ E within Eastern Kamchatka approximately 340 km northeast of Petropavlovsk-Kamchatsky. It is a Hawaiian type volcano, belonging to the southern part of the Klyuchevskaya volcano group, which is one of the world-known volcanic areas with recent volcanic activity. It has some features, which discriminate it from typical subduction-zone volcanoes, first of all by high alkali contents (up to 7 wt.% $Na_2O + K_2O$) and great depth (180-190 km) of the subducting slab beneath the volcano (Gorbatov et al. 1997). The age of the Tolbachik volcano is 10,000 years (Braitseva et al. 1995). From July 1975 to December 1976, a fissure eruption took place in the southern part of the Plosky Tolbachik, which was called as “the Great Tolbachik Fissure Eruption” and studied in detail (e.g., Fedotov and Markhinin 1983).

The volcanic activity in this area resumed on November 27, 2012 and continued until October 2013. The lava flows formed three fields during this stage of eruption, more than 10 km long, with an average thickness of 20 m (Fig. 1). The Vodopadnoye field has its source from the Menyailov vent; it was formed within the first two days, and by November 29, 2012 it was 8.5 km long and 5.65 $km^2$ in size (Dvigalo et al. 2017). The second, Leningradskoye field was formed from the Naboko vent. It is an interbedding of numerous lava flows and pyroclasts (ashes, scoria, and volcanic bombs). Its thickness varies from 69 m near the source to 5-15 m at the distal end. The third field, Toludskoye, sourced from

the same long-lived Naboko vent, started forming on December 22-23, 2012, and by June 5, 2013, reached the length of 4.26 km with the maximal width of 3.8 km at the front and the thickness of up to 53 m. The maximal activity of the eruption was from December 2012 to February 2013, when more than ten volcanic vents were active. Exactly within this period, the southern foot of the Plosky (Flat) Tolbachik volcano was covered by a great amount of pyroclastic material, in which diamonds were identified (Fig. 2).

**Sampling**

On December 12, 2012, two samples of basaltic lavas, approximately 1 kg in weight were collected in the western part of the fresh Leningradskoye lava flow for a study of accessory minerals in basaltic lavas. The rocks in this flow are black aphyric basalts with a porous cinder crust filled in with pyroclastic material. Approximately 500 small grains of diamond were identified from the powdery white coating of deltalumite (tetragonal polymorph of $Al_2O_3$; Pekov et al. 2016) on the lava samples. This coating was unusual for the lavas and, in fact, that was the reason why the samples were collected from that part of the lava flow. The mineralogical analysis of the samples was performed in the laboratory of the Institute of Volcanology and Seismology, Russian Academy of Sciences using standard techniques: hand crushing, sieving, panning, electromagnetic and sometimes heavy liquid separations. The diamonds were found in the coating deltalumite material, which was falling off the lava samples without the use of any metallic tools. Of particular interest is a recent find by one of the authors (LPA) of an *in situ* association of diamond with deltalumite, from the ash of another Kamchatka volcano, Koryakskii, where a microcrystal of diamond overgrows the surface of the rounded deltalumite grain (Fig. 3). Both diamond and deltalumite were identified with the use of EDX spectra.

The identification of diamond grains in the samples was unexpected, and more than 50 samples of fresh, hot volcanoclastic material from the southeastern end of the Naboko vent were collected in February 2013, in order to check the initial diamond finds. Several tens more diamonds of the similar size

and morphology were found. Subsequently, single diamond grains were found in two samples collected from the lava flow of the Toludskoye lava field and to the east of that field, as well as three diamonds from a sample, approximately 10 kg in weight, collected in 1975 from the old flow. The total number of diamond grains exceeds now 700.

**Secondary ion mass spectrometry (SIMS) measurements**

The measurement of impurity elements in Tolbachik diamond #1 was carried out by using a mass spectrometer Cameca IMS-4f. This method is well known and consists of using $Cs^+$ primary ions for detection of negative secondary ions or $O_2^+$ primary ions for detection of positive secondary ions. Element distribution maps were acquired using Dynamic Transfer System (DTS). The mass spectral resolution of 5,000 was used to overcome interference problems. Lateral resolution was determined by the field-of-view aperture and equals 5 μm with a raster of 250 × 250 μm. Concentrations of impurity elements in diamond, in at/cm$^3$, were calculated on the basis of the Relative sensitivity factors (Wilson, 1995).

Two other diamonds (## 2 and 3) from Tolbachik have been investigated with the Cameca IMS1280-HR mass spectrometer.

**Infrared spectroscopy (FTIR)**

IR spectra were obtained with the use of FTIR spectrometer Nicolet 380 with a microscope Centarius THERMO Electron corporation. The resolution of spectra was 4-6 cm$^{-1}$ after 100-200 runs. The nitrogen calculation was performed using the method proposed by Taylor et al. (1996).

**Electron microscopy**

Transmission electron microscopy (TEM) was performed at the Helmholtz Centre Potsdam to study the internal structure of diamonds, the existence and compositions of mineral inclusions in them.

Five diamonds from Tolbachik have been investigated with TEM (T1, T2, T3, TOP, and CH). For the TEM use, two foils were prepared by FIB technique from each diamond; one from the centre of the crystal and another one from the rim part. From the centre of sample CH, we prepared two foils. In total, 11 foils were produced. The TEM foils were sputtered from the host diamond using a HELIOS G4UC focused ion beam system operating at GFZ Potsdam. Foil sizes were approximately 15 × 10 × 0.1 μm. Details of the FIB sample preparation are presented elsewhere (Wirth 2004, 2009). The foil numbers are: #5575 – from T1 centre, #5576 - from T1 rim; #5577 - from T2 centre, #5578 - from T2 rim; #5581 - from T3 centre, #5582 - from T3 rim; #5583 - from TOP centre, #5584 - from TOP rim; #5579 and #5599 - from CH centre; #5580 - from CH rim.

The TEM foils with an average thickness of approximately 100 nm were studied using a TECNAI F20 transmission electron microscope operated at 200 keV with a Schottky field emitter as an electron source. The TEM is equipped with a Gatan electron energy loss spectrometer (EELS) Tridiem™, and EDAX X-Ray analyzer with ultrathin window and a Fishione high-angle annular dark field detector (HAADF). HAADF images were acquired either with a camera length of 75 mm resulting in Z-contrast imaging or with 330 mm camera length providing Z-contrast and diffraction contrast. EDS X-ray analyses usually were performed in the scanning transmission mode (STEM) scanning the electron beam within a preselected window. The size of the window was adapted to the size of the object of interest to be measured. Counting time usually was 60 seconds to accumulate enough counts above background for reliable counting statistics.

The chemical compositions of mineral inclusions in diamonds were always measured in the scanning transmission mode (STEM) thus avoiding significant mass loss during data acquisition. Acquisition time was 60 or 120 seconds. Data evaluation occurred using the TIA software package of the microscope.

Some EDX spectra were obtained with the use of scanning electron microscope Tescan Mira LMU, equipped with energy dispersive X-ray spectroscopy X-Max 50 (Oxford Instruments), which worked at a beam voltage 20 kV and current 20 nA.

### Isotope analysis

Isotope compositions of carbon and nitrogen were performed with the use of the Cameca IMS1280-HR mass spectrometer. Two reference diamonds were used, the JWH diamond and the Cameca diamond. The characteristics of the JWH diamond are as following: $\delta^{13}C_{VPDB}$ = -25.577 ± 0.039 ‰; $\delta^{15}N_{Air}$ = +21.2 ± 0.6 ‰; N-content = 225 ± 3 ppm. The Cameca reference diamond has $\delta^{13}C_{VPDB}$ = -52.32 ‰. $Cs^+$ion bombardment intensity was 10 keV for carbon and 20 keV for nitrogen. Both datasets, obtained on the two reference samples, demonstrate that precision was less than 0.2 ‰.

## RESULTS

### Crystal morphology and internal structure

The diamond grains are 0.06-0.7 mm in size (i.e., they may be called microdiamonds) and are colorless to yellow-green in color (Fig. 4). They are accompanied, in samples, with single grains of moissanite, milky-white corundum, various spinellides, sulfides, Cu-Sn alloys, and native iron, aluminum, and copper.

Morphologically most crystals of diamond are isometric, combination-type cube-octahedra (Fig. 4). Some crystals are spinel-type (111) and Moos-Rose (001) twins. A diffraction pattern of some diamonds is typical of twinned crystals, indicating microtwinning within diamond crystals (Gordeev et al. 2014). Cubic faces frequently bear square-pyramidal etch-pits; some crystals show zonation in cathodoluminescence. Such crystals are characteristic for Tibetan chromitites, French Guyana komatiites,

lamprophyres of Northern Quebec, and can be observed in kimberlites worldwide (Litasov et al. 2019; McCandless et al. 1999; Orlov 1987).

According to TEM analyses, the studied diamonds from the Tolbachik volcano, in contrast to diamonds from kimberlites and placer deposits, are extremely homogeneous (Fig. 5A). They virtually lack stacking faults, dislocations, low-angle grain boundaries and cracks, characteristic for most natural diamonds. Only the central part of diamond T1 contains a few stacking faults with partial dislocations, which are characteristic for stacking faults (Fig. 5B). The other diamonds contain only singular cracks.

Mineral inclusions of metal alloys and silicides in diamonds have oval shapes and sizes of 70-450 nm, sometimes with nano-pores in their peripheral parts (Figs. 5C,D). The particles of the same composition occur on the diamond surfaces (Fig. 6A) and on the surfaces of volcanic ash particles (Fig. 6B).

**Distribution of impurity elements in diamonds**

Fig. 7 demonstrates the distribution of impurity elements in diamond # 1, obtained with use of a Cameca IMS-4f mass spectrometer. Two groups of impurity elements can be distinguished based on their distribution within the diamond. (1) The first group of elements, N and H, the most common structural impurities in diamond, are distributed, within the crystal, like C, homogeneously (Fig. 7A,B,C).(2) All other elements (Cl, F, O, S, Si, Al, Ca, and K) form local concentrations, exceeding the background by 1-4 orders of magnitude (Fig. 7D,E,F), implying the existence of inclusions, causing such relatively high concentrations of these elements. High concentrations of some ‘elevated’ elements (e.g., O, F, and Cl) coincide with each other, demonstrating their connection in forming some mineral inclusions.

Table 1 and Fig. 8 show the content of impurity elements in a Tolbachik diamond, their concentrations and distribution.

The concentration of nitrogen in sample 1 is 304 ppm, similar to determinations in samples 2 and 3 with the use of Cameca IMS 1280-HR (97 ppm and 288 ppm; Table 3), i.e., the diamonds are low-nitrogen varieties of Group 2a (Kaminsky and Khachatryan 2001).

The concentration of hydrogen, calculated in diamond #1on the basis of the relative sensitivity factors (Wilson 1995), is 526 ppm, while in diamond #2 it is 289 ppm. These figures may be considered only as tentative. During the course of the SIMS analysis, in the analytical chamber, high vacuum (~3 × $19^{-9}$ Torr) exists. However, some remaining gases, such as $H_2O$ may occur on the internal chamber surface, and create a background of H (as well as O) that is difficult to valuate. Without heating the chamber, the adsorbed water cannot be removed from the surface.

Oxygen, although possibly overvalued for the same reason, also shows elevated concentrations, over 7,000 ppm (Table 1). Most of O occurs as local concentrations, coinciding with concentrations of F and Cl (Fig. 7). The O background is also high, 2,000-5,000 ppm. It may form C-O and/or H-O aggregations.

In addition to N and H, which are major structural impurities in diamond, F, Cl, Na and Si have relatively elevated contents that are caused, most likely, by their concentrations in micro- and nanoinclusions along with O. The calculated F/Cl mass ratio in the diamond is 0.39 (Table 1), which is almost identical to the average F/Cl ratio in volcanic gases from the Tolbachik eruption in 2013 (0.365; Zelenski et al. 2014) and almost one order of magnitude higher than in volcanic gases from persistently degassing subduction-zone volcanoes (0.076; Shinohara 2013). Volcanic gases from Tolbachik are also enriched in Na (Zelenski et al. 2014; Chaplygin et al. 2016).

Fig. 8 demonstrates the distribution of admixture elements in diamond 1, in comparison with the distribution of elements in volcanic gases from Tolbachik, collected in the vicinity of the hot lava flow in 2013 (Zelenski et al. 2014). One can see that the patterns of the two distributions are similar, particularly for volatiles (F and Cl).

It can be seen that in addition to the silicate inclusions, volatile elements show increased concentration. It is interesting that the F/Cl ratio in the studied diamonds almost coincides with the value

of this ratio measured in the volcanic gas. These data indicate the relationship between the mechanism of formation of these diamonds and the gas phase.

## Nitrogen in diamonds

A typical FTIR spectrum of a Tolbachik diamond is presented in Fig. 9.

In addition to the diamond's own absorption bands, within the 1800-4000 $cm^{-1}$ range, only single-atom nitrogen C-center bands within 1000-1400 $cm^{-1}$ cm occur, as well as bands within 3000-4000 $cm^{-1}$ and 1300-1700 $cm^{-1}$. The 1300-1700 $cm^{-1}$ band, most likely, is caused by hydrogen (O-H or N-H) bending motions. The concentrations of single-atom nitrogen (which is the total nitrogen content) in the studied Tolbachik diamonds are shown in Table 2.

The average nitrogen concentration in the studied samples is 233.8 ±143.8 (2σ), i.e., similar to the results obtained from the IMS analyses (see Tables 1 and 3).

By their IR characteristics, the Tolbachik diamonds are similar to the both diamonds synthesized in the metal-carbon system (Palyanov et al. 1997), natural 'metamorphic' microdiamonds from Kazakhstan (Khachtryan 2013), and microdiamonds from Tibetan and Uralian chromitites (Xu et al. 2017). In any case, IR data demonstrate fast, short-time recent origin of the studied Tolbachik diamonds with almost no residence time at high temperatures (Taylor et al. 1996).

## Isotopic compositions of C and N in diamonds

Carbon isotopic compositions in diamonds 2 and 3 from the Tolbachik volcano, according to SIMS analyses with the use of Cameca IMS 1280-HR, are -26.73 ‰ and -28.66 ‰ $\delta^{13}C_{VPDB}$ (Table 3). These results are similar to the data obtained earlier by Karpov et al. (2014) and Galimov et al. (2016a), which lay within the range from -22 ‰ to -27 ‰ $\delta^{13}C_{VPDB}$ with an average -25.4 ± 1.2 ‰ $\delta^{13}C_{VPDB}$ (Fig. 10).

Similar compositions are characteristic for dispersed carbon in lavas of the Tolbachik 2012-2013 eruption with an average $\delta^{13}C_{VPDB}$ = -26.8 ± 1.1 ‰ (Galimov et al. 2016a).

Nitrogen isotopic compositions in diamond from Tolbachik volcano, determined also with the use of Cameca IMS 1280-HR, are -2.58 ‰ and -2.32 ‰ $\delta^{15}N_{Air}$, with the N-contents in these samples, are 97.65 and 288.99 ppm respectively (Table 3). Such N-isotopic compositions fit all major diamond varieties (peridotitic, eclogitic and lower-mantle diamonds), with the exception of 'metamorphic' diamonds (Cartigny and Busigny 2018).

The combined C-N isotopic composition of the studied Tolbachik diamonds corresponds to the eclogitic-type association in kimberlites and lamproites (Kaminsky 2011) (Fig. 11). Similar compositions, with $\delta^{15}N_{Air}$ down to −3.4‰ are observed for volcanic gases from the Mutnovsky volcano, South Kamchatka (Zelenski and Taran 2011).

If the Tobachik diamonds were synthetic, their $\delta^{15}N_{Air}$values would be atmospheric (at 0).

**Mineral inclusions**

Mineral inclusions in the studied diamonds are small (70-450 nm in size), round- or oval-shaped grains (Figs. 5C,D). They form a paragenetic association with Tolbachik diamonds. According to EDX data, the inclusions are represented by two mineral groups: Mn-Ni alloys and silicides (Table 4 and Fig. 12). Within each group, wide variations exist. Alloys vary in stoichiometry from MnNi to $Mn_2Ni$, with a minor admixture of Si from 0 to 5.20-5.60 at.%. This group is close to the Mn-rich part of Group 1 Mn-Ni-Si-Fe alloys identified earlier in diamond crystallites from the Avacha volcano (Kaminsky et al. 2016). It is possible, that the minor Si concentrations in some alloys, may be caused by the silicide phase, which might be underneath. Silicides, usually coexisting with alloys, vary in composition from $(Mn,Ni)_4Si$ to $(Mn,Ni)_5Si_2$ and $Mn_5Si_2$, and further to MnSi, forming pure Mn-silicides. The compositional field of

279 silicides occupies the Mn-rich part of Group 2 Mn-Ni-Si-Fe alloys identified earlier in diamond
280 crystallites from the Avacha volcano (Kaminsky et al. 2016).

281 A characteristic feature of the inclusions is their polyphase structure: their central, early phase is
282 usually an alloy (bright in Figs. 5C and 5D), on which silicide (gray in Figs. 5C and 5D) is developed. In
283 Fig. 12, coexisting compounds are shown as dotted lines with numbers of diamond samples, in which
284 they were analyzed.

285 Each mineral inclusion grain has nanometer-sized pores, 20-30 nm in size, usually in the periphery
286 of grains, that might have contained or still contain a fluid or a gas phase (Figs. 5D and Fig. 13A).
287 According to EDX spectra obtained from the inclusions, the pores contain chlorine, fluorine, and oxygen
288 in their compositions (Fig. 13B). Unfortunately, we were unable to quantify chlorine, fluorine, and
289 oxygen because there are no reliable $k_{AB}$ factors available to calculate the concentration of these elements.
290 (The $k_{AB}$ factor is a factor in the Cliff-Lorimer equation $C_a/C_b = k_{AB} I_a/I_b$, where $C$ are the weight fractions
291 of the two elements in question, and $I$ are the measured characteristics X-ray intensities (Cliff and
292 Lorimer 1975).

293 In order to study compositions of nanoinclusions in diamond #1, we performed the EDX analyses
294 of two inclusions in Tolbachik diamond 2 with the use of scanning electron microscope X-Max 50
295 Oxford Instruments (Fig. 14). In their spectra, on the background of carbon peak from the host diamond
296 (Fig. 14B), Mn and Si peaks (major), as well as O and F peaks occur, characterizing the inclusion
297 composition (Fig. 14C,D). The inclusions are, most likely, silicides, similar to those identified with the
298 use of EDX-TEM data, and particularly to Mn-silicides in grains 1a from sample T1-centre and 2 in
299 sample T1-rim (see Table 4). Of particular interest is the admixture of fluorine in these inclusions, which
300 is characteristic to both diamonds and gases from the Tolbachik volcano (Table 1). Possibly, they fill
301 nano-pores in silicides (Fig. 5D).
302
303 **DISCUSSION**
304

**Contamination or growth in the natural environment?**

The artificial origin of the studied diamonds should be excluded because no drilling operation or any other industrial activities were performed in this area, and no diamond-bearing instruments have been used during the sampling and sample preparation process. The most important proof of a natural origin of diamonds in Tolbachik and other Kamchatka volcanoes is a recent find *in situ* association of diamond with deltalumite, in the Koryakskii volcano (Anikin et al. 2018) in which a microcrystal of diamond overgrows the surface of the rounded deltalumite grain (Fig. 3).

The geological data demonstrate that Tolbachik diamonds are generally related to pyroclastic material of the Tolbachik fissure eruption, which was closely related to its gaseous activity. As a consequence, Tolbachik diamonds are enriched in volatiles, first of all in F and Cl by 2-3 orders of magnitude compared to other admixture elements - exactly like volcanic gases collected during the course of the eruption (Fig. 6). Not only diamonds, but also virtually all inclusions have in their peripheral parts small pores, containing fluorine and chlorine, which are characteristic for processes of volcanic eruptions (Zelensky and Taran 2011; Zelensky et al. 2014).

The major structural impurity element in diamond, nitrogen has concentrations at ~300 ppm, higher than in artificial diamonds (McNamara 2003; Kazuchita et al. 2016). Its isotopic characteristics are -2.58 ‰ and -2.32 ‰ $\delta^{15}N_{Air}$, different from artificial diamonds, in which isotopic composition is of the air's nitrogen, 0 ‰.

The most common mineral inclusions within the studied diamonds, which form their paragenetic association, are Mn-Ni alloys with outgrowth silicides, that is not characteristic for processes of diamond synthesis (Bezrukov et al. 1972). The analogous Fe-Ni alloys were identified as inclusions even in the Earth's deep mantle (Smith et al. 2016). Non-industrial origin of these inclusions is confirmed by their finds not only inside diamonds, but also on their surfaces (Fig. 6A) and even on surfaces of volcanic ash particles (Fig. 6B).

Some researchers consider the existence of Mn-Si inclusions in diamonds as the main evidence of their synthetic origin (Litasov et al. 2019). Indeed, inclusions of Fe-Ni-Mn-Co alloys in Tolbachik diamonds are remeniscient of catalysts for the artificial manufacturing of HPHT diamonds. They usually have $Mn_{60}Ni_{40}$ composition, which corresponds to the eutectic at 1 atm and 1020 ˚C. However, the inclusions in Tolbachik diamonds are radically different. Firstly, they have very variable compositions, different of the eutectic: from MnNi to $Mn_2Ni$ with 45-67 at.% of Ni (see Table 4). Secondly, they contain up to 5 at.% of Si, which is never used for man-made diamonds (Palyanov et al. 1997). Earlier, in diamonds from another Kamchatka volcano, Avacha, we found inclusions of alloys with Si up to 19 at.% (Kaminsky et al. 2019). Thirdly, inclusions of alloys in Tolbachik diamonds are associated with silicides, which overgrow alloys (see Fig. 5). The silicides have very variable compositions: from $(Mn,Ni)_4Si$ to $(Mn,Ni)_5Si_2$ and $Mn_5Si_2$, and further to MnSi, forming pure Mn-silicides (see Table 4). Silicides never occur in synthetic diamonds (Lang et al. 1995), but frequently exist in volcanic ashes (Karpov et al. 2017b). The analogous association of alloys and silicides, with even wider variations in their compositions, occurred in polycrystalline diamond aggregates from the Avacha volcano and Koryakia, both in Kamchatka (Kaminsky et al. 2016, 2019) (see Fig. 12).

The analogous problem appeared for the understanding of the natural origin of diamonds in Tibetan ophiolites because of their cube-octahedral morphology, yellow color due to unaggregated nitrogen, metal-alloy inclusions and highly negative $\delta^{13}C$ values, - like in the studied Tolbachick diamonds. However, higher concentrations of trace elements, high range of $\delta^{15}N$ (up to -5.6 ‰), like in the studied diamonds, indicate their natural origin (Howell et al. 2015). The unaggregated nitrogen suggests a short history of the Tolbachik diamonds and lack of their residence under high temperatures (Taylor et al. 1996). This requires a new understanding of their origin.

## Model of origin of Tolbachik diamonds

**Place and time of origin.** The geological and tectonic setting of Tolbachik diamonds obviously rules out a possibility of stable high *P-T* conditions of their formation, characteristic for 'classical' diamonds from kimberlites and lamproites. Most likely, they were formed, along with other accessory minerals (moissanite, corundum, native metals) within the powdery coating on lava, from the magmatic gas-fluid system. Not occasionally, the Tolbachik eruption 2012-2013 was highly gas saturated; and the ashes of the new eruption contain higher Cu, Co, and Ga contents in comparison to lavas (Gordeev et al. 2014).

Karpov et al. (2014) found a very interesting detail on Tolbachik diamonds: a series of various minerals and microfilms coating the diamond crystals. There are, among these minerals, silicates, alumosilicates, sulfates, and oxides. These minerals have high concentrations of Fe, Ni, and Cu, and some silicates contain nano-inclusions of Ni-Cu and Cu-Sn alloys, analogues to inclusions in diamonds. These characteristic features of Tolbachik diamonds correspond to chemical features of minerals observed in pores of solidified diamond-bearing lavas and in volcanic ashes. They confirm the close relationship of the observed diamonds to the volcanic process.

The Tolbachik diamonds may have been formed during the explosive phase of the eruption process and comprise pores located between their inclusions and host material. These pores in diamond are filled in with an F-Cl gaseous material, characteristic for volcanic eruption processes.

The finding of diamond at the surface of rounded deltalumite grain, overgrowing it (Fig. 3), indicates the simultaneous origin of these minerals during the activity of volcanic gases and their formation along with volcanoclastic material.

**Source of carbon**. Carbon isotopic compositions of Tolbachik diamonds were carried out in three different laboratories with the use of different techniques: gas mass spectrometers Delta V Advantage (Karpov et al. 2014) and Delta Plus (Galimov et al. 2016a), and SIMS (Cameca IMS1280-HR) for our new data. The values of $\delta^{13}C$ from all laboratories are within the range from -22 ‰ to -29‰ with an average at -25.4 ‰ $\delta^{13}C_{VPDB}$. This range is similar to the composition of carbonado diamonds (which have crustal sources of carbon) and, more important, fully coincides with the isotopic composition of

carbon in lavas of the Tolbachik 2012-2013 eruption (Galimov et al. 2016a). Moreover, these values are similar to the isotopic compositions of hydrocarbons from the Uzon Caldera, Kamchatka (Galimov et al. 2015). This data allows us to conclude that the volcanic gases that participated in the Tolbachik eruption, were the source of the carbon in Tolbachik diamonds.

**Conditions of origin**. The occurrence, in the Tolbachik lavas, of a diamond in association with moissanite and native Fe, Al, and Cu, indicates the highly reduced conditions of their formation. According to experimental and empirical data, the formation of moissanite only occurs at an oxygen fugacity at 5–7.5 log units below the iron-wüstite buffer (IW), more reducing than the present-day mantle redox state and does not need high pressure (Schmidt et al. 2014; Shiryaev and Gallard 2014; Golubkova et al. 2016). Native metals and alloys occur in peridotites and chromitites (including diamondiferous ones), which ultra-high pressure (UHP) origin is debatable (Pujol-Sol et al. 2018; Economou-Eliopoulos et al., 2019; Farré-de-Pablo, 2019). Studying such assemblages in various tectonic environments, Griffin et al. (2018) interpret them as reflecting the interaction between basaltic melts and mantle-derived fluids dominated by $CH_4 + H_2$.

**Mechanism of origin**. Enrichment of the studied Tolbachik diamonds in volatiles implies their genetic relationship to volcanic gases; their small sizes and unusually homogeneous internal structure suggest their very fast crystallization. The presence, in the Tolbachik diamonds, of only a single-atom, non-aggregated nitrogen impurity also demonstrates their fast, short-time origin, as well as almost no residence time at high temperatures.

For the studied earlier polycrystalline diamonds from the Kamchatka volcanoes in similar environments, the CVD formation was suggested (Kaminsky et al. 2016, 2019). In contrast to those polycrystalline diamonds, the monocrystalline diamonds from Tolbachik do not bear microtwinning and lattice defects, which are characteristic for CVD diamonds (Shechtman et al. 1993; Klages and Schäfer 1998; Butler and Oleynik 2008). This leads us to the possibility of an alternative, cavitation model of the origin of the Tolbachik diamonds, which was offered by Galimov (1973) and proven experimentally (Galimov et al. 2004). Cavitation is a process, in which high pressures and temperatures occur at several

407 points, whereas the ambient parameters are, on average, moderate. It occurs in fluids containing dissolved
408 gases, and high gas contents are necessary conditions for the formation of diamond (Galimov 1973).
409 Deposition of diamond and graphite from gas ($CH_4$) during the epitaxy process is accompanied by
410 significant carbon isotope fractionation. In experiments with the epitaxial synthesis of diamond ($T$ =
411 1050°C; $P$ = 0.02 Torr, initial gas $CH_4$, and by using the cyclic etching procedure, following V. Deryagin
412 and D. Fedoseev's method) overgrowing diamond was enriched in the heavy carbon isotope with
413 $\delta^{13}C_{VPDB}$ = -22 to -26 ‰, while co-existing graphite was enriched in the light carbon isotope with
414 $\delta^{13}C_{VPDB}$ = -65 to -67 ‰ relative to the initial $CH_4$ with $\delta^{13}C_{VPDB}$ = -46.2 ‰ (Galimov 1973). In contrast
415 to the epitaxy mechanism, cavitation synthesis is not accompanied by the isotope fractionation (Galimov
416 et al. 2004).
417
418 **IMPLICATIONS**
419
420 Diamonds from the Tolbachik volcano in Kamchatka are very specific in their internal structure,
421 impurity elements, carbon and nitrogen isotopic compositions, and mineral inclusions. They have cube-
422 octahedral shape and extremely homogeneous internal structure. Nitrogen and hydrogen, the most
423 common structural impurities in diamond, are distributed homogeneously. Of particular interest is the
424 F/Cl ratio in the studied diamonds, which almost coincides with the value of this ratio measured in the
425 volcanic gas. This indicates a close relationship between the mechanism of formation of these diamonds
426 and the gas phase and demonstrates a possibility of crystallization of diamond from gas in the natural
427 environment.
428 Mineral inclusions in the studied diamonds from Tolbachik are 70-450 nm in size, round- or oval-
429 shaped grains. They are represented by two mineral groups: Mn-Ni alloys and silicides, with wide
430 variations for each group. The mineral inclusion grains have nano-sized pores that contain a fluid or a gas
431 phase (F and O) that also confirm the close relationship of the diamonds and volcanic gases.

Carbon isotopic compositions in diamonds vary within the range from -21 ‰ to -29 ‰ $\delta^{13}C_{VPDB}$ (av. = -25.4). Nitrogen isotopic compositions in diamond from Tolbachik volcano are from -2.32 ‰ to -2.58 ‰ $\delta^{15}N_{Air}$. These parameters are quite specific for diamonds.

The geological, geochemical and mineralogical data confirmed the natural origin of studied Tolbachik diamonds from volcanic gas, most likely, as a result of cavitation mechanism at the extremely powerful explosive phase of the eruption. These diamonds demonstrate polygenesis of diamond in the natural environment.

## ACKNOWLEDGEMENTS

The authors are thankful to Dr. P. Peres (Cameca, Gennevilliers, Paris, France) and Dr. I. Fedik (AMETEC, Moscow, Russia) for their assistance in analytical work, and Prof. Yu. A. Litvin (IEM RAN, Chernogolovka, Russia) for fruitful discussions.

The work was partly supported by the Russian Foundation for Basic Research (RFBR), grant № 19-05-00554\19.

## REFERENCES CITED

Anikin, L.P., Sokorenko, A.V., Ovsyannikov, A.A., Sidorov, E.G., Dunin-Barkovsky, R.L., Antonov, A.V., and Chubarov, V.M. (2014) A find of diamonds in lavas from the Tolbachik eruption 2012-2013. In: Volcanism and related processes, IVO DVO RAN, Petropavlovsk-Kamchatsky, 20-23 (in Russian).

Anikin, L.P., Silaev, V.I., Chubarov, V.M., Petrovsky, V.P., Vergasova, V.P., Karpov, G.A., Sokorenko, A.V., Ovsyannikov, A.A., and Maximov, A.P. (2018) Diamond and other accessory minerals from the Koryakskii volcano (Kamchatka) eruption 2008-2009. Vestnik Institute of Geology, Komi Scientific Center, RAN, No. 2, 18-27 (in Russian).

458 Baikov, A.I., Anikin, L.P., and Dunin-Barkovsky, R.L. (1995) Find of carbonado in volcanic rocks of
459 Kamchatka. Doklady AN SSSR 343(1), 72-74 (in Russian).
460 Bezrukov, G.N., Butuzov, V.P., Khatelishvili, G.V., and Chernov, D.B. (1972) Study of compositions in
461 crystals of synthetic diamonds with the use of local analysis method. Doklady AN SSSR 204(1),
462 84-87 (in Russian).
463 Braitseva, O.A., Melekestsev, I.V., Ponomareva, V.V., Sulerzhitsky, L.D., and Litasova, S.N. (1995)
464 Ages of active volcanoes in the Kuril-Kamchatka region. Volcanology and Seismology 16(4-5),
465 341-370.
466 Butler, J.E., and Oleynik, I. (2008) A mechanism for crystal twinning in the growth of diamond by
467 chemical vapour deposition. Philosophical Transactions of the Royal Society A 366, 295–311. DOI:
468 10.1098/rsta.2007.2152.
469 Cartigny, P., and Busigny, V. (2018) Nitrogen Isotopes. In: W. White, W.H. Casey, B. Marthy, H.
470 Yurimoto (Eds.) Encyclopedia of Geochemistry, Springer, pp. 991-1003.
471 Chaplygin, I.V., Lavrushin, V.Y., Dubinina, E.O., Bychkova. Y.V., Inguaggiato, S., Yudovskaya, M.A.
472 (2016) Geochemistry of volcanic gas at the 2012-2013 New Tolbachik eruption, Kamchatka.
473 Journal of Volcanology and Geothermal Research 323, 186-193. DOI:
474 10.1016/j.jvolgeores.2016.04.005.
475 Cliff, G., and Lorimer, G.W. (1975) The quantitative analysis of thin specimens. Journal of Microscopy
476 103(2), 203-207. DOI: 10.1111/j.1365-2818.1975.tb03895.x.
477 Dvigalo, V.N., Svirid, I.Yu., and Shevchenko, A.V. (2017) Quantitative evaluations of parameters of the
478 Fissure Tolbachik eruption 2012-2013 according to data of aerophoto observations. In: Fissure
479 Tolbachik eruption 2012-2013. Sibirsky Branch of Russian Academy of Sciences Publishing
480 House, Novosibirsk, pp. 91-108 (in Russian).
481 Economou-Eliopoulos, M., Tsoupas, G., and Skounakis, V. (2019) Occurrence of graphite-gike carbon in
482 podiform chromitites of Greece and its genetic significance. Minerals 9, 152-160.

Farré-de-Pablo J., Proenza J.A., González-Jiménez J.M., Garcia-Casco A., Colás V., Roqué-Rosell J., Camprubí A., and Sánchez-Navas A. (2019) Diamonds in ophiolitic chromitites are not in all cases formed at UHP conditions. Goldschmidt Abstracts, 955.

Fedotov, S.A., and Markhinin, Ye.K. (Eds.) (1983) The Great Tolbachik Fissure Eruption: Geological and Geophysical Data, 1975-1976. Cambridge University Press, Cambridge, London e.a., 341 pp. DOI: 10.1017/S0016756800028119.

Galimov, E.M. (1973) On possibility of natural diamond synthesis under conditions of cavitation, occurring in a fastmoving magmatic melt. Nature 243, 389–391.

Galimov, E.M., Karpov, G.A., Sevast'yanov, V.S., Shilobreeva, S.N., and Maksimow, A.P. (2016a) Diamonds in the products of the 2012–2013 Tolbachik eruption (Kamchatka) and mechanism of their formation. Geochemistry International 54(10), 829–833. DOI: 10.1134/S0016702916100037.

Galimov, E.M., Kudin, A.M., Skorobogatskii, V.N., Plotnichenko, V.G., Bondarev, O.L., Zarubin, B.G., and Strazdovskii, V.V., Aronin, A.S., Fisenko, A.V., Bykov, I.V., and Barinov, A.Yu (2004) Experimental corroboration of the synthesis of diamond in the cavitation process. Doklady Earth Sciences 49(3), 150–153.

Galimov, E.M., Prokhorov, V.S., Fedoseev, D.V., and Varnin, V.P. (1973) Heterogenic carbon isotopic effects during the course of synthesis of diamond and graphite from gas. Geochemistry 1973(3), 416-424 (in Russian).

Galimov, E.M., Sevast'yanov, V.S., Karpov, G.A., Kamaleeva, A.I., Kuznetsova, O.V., Konopleva, I.V., and Vlasova, L.N. (2015) Hydrocarbons from a volcanic area. Oil seeps in the Uzon caldera, Kamchatka. Geochemistry International 53(12), 1019–1027. DOI: 10.1134/s0016702915120046.

Galimov, E.M., Sevastyanov, V.S., Karpov, G.A., Shilobreeva, S.N., and Maksimov, A.P. (2016b) Microcrystalline diamonds in the oceanic lithosphere and their nature. Doklady Earth Sciences 469(1), 670–673. DOI: 10.1134/S1028334X16070011.

Golubkova, A., Schmidt, M.W., and Connolly, J.A. (2016) Ultra-reducing conditions in average mantle peridotites and in podiform chromitites: A thermodynamic model for moissanite (SiC) formation. Contributions to Mineralogy and Petrology, 171(5), 41.DOI: 10.1007/s00410-016-1253-9.

Gorbatov, A., Kostoglodov, V., Suárez, G., and Gordeev, E. (1997) Seismicity and structure of the Kamchatka subduction zone. Journal of Geophysical Research 102, 17883–17898. DOI: 10.1029/96JB03491.

Gordeev, E.I., Karpov, G.A., Anikin, L.P., Krivovichev, S.V., Filatov, S.K., Antonov, A.V., and Ovsyannikov, A.A. (2014) Diamonds in lavas of the Tolbachik fissure eruption in Kamchatka. Doklady Earth Sciences 454(1), 47–49.DOI: 10.1134/S1028334X14010097.

Griffin, W.L., Huang, J.-X., Thomassot, E., Gain, S.E.M., Toledo, V., and O'Reilly, S.Y. (2018) Super-reducing conditions in ancient and modern volcanic systems: sources and behaviour of carbon-rich fluids in the lithospheric mantle. Mineralogy and Petrology 112, 101-114. DOI: 10.1007/s0071.

Howell, D., Griffin, W.L., Yang, J., Gain, S., Stern, R.A., Huang, J.-X., Jacob, D.E., Xu, X., Stokes, A.J., O'Reilly, S.Y., and Pearson. N.J. (2015) Diamonds in ophiolites: Contamination or a new diamond growth environment? Earth and Planetary Science Letters 430, 284–295. DOI: 10.1016/j.epsl.2015.08.023.

Kaminsky, F.V. (2011) Mineralogy and Geochemistry of the Lower Mantle. Moscow, GEOHI, 68 pp. (in Russian).

Kaminsky, F.V., and Khachatryan, G.K. (2001) Characteristics of nitrogen and other impurities in diamond, as revealed by infrared absorption data. Canadian Mineralogist 39(6), 1733-1745.

Kaminskiy, F.V., Patoka, M.G., and Sheymovich, V. S. (1979) Geologic and tectonic position of diamond-bearing basalts of Kamchatka. Doklady Earth Science Sections 246, 55-58.

Kaminsky, F.V., Wirth, R., Anikin, L.P., Morales, L., and Schreiber, A. (2016) Carbonado-like diamond from the Avacha active volcano in Kamchatka, Russia. Lithos, 265, 222-236. DOI: 10.1016/j.lithos.2016.02.021.

533 Kaminsky, F.V., Wirth, R., Anikin, L.P., and Schreiber, A. (2019) 'Kamchatite' diamond aggregate from
534 northern Kamchatka, Russia: New find of diamond formed by gas phase condensation or chemical
535 vapor deposition. American Mineralogist 104(1), 140-149. DOI: 10.2138/am-2018-6708.
536 Karpov, G.A., Silaev, V.I., Anikin, L.P., Rakin, V.I., Vasil'ev, E.A., Filatov, S.K., Petrovskii, V.A., and
537 Flerov, G.B. (2014) Diamonds and accessory minerals in products of the 2012–2013 Tolbachik
538 fissure eruption. Journal of Volcanology and Seismology 8(6), 323–339.DOI:
539 10.1134/S0742046314060049.
540 Karpov, G.A., Silaev, V.I., Anikin, L.P., Mokhov, A.V., Gornostayeva, T.A., and Sukharev, A.E. (2017)
541 Explosive mineralization. In: Tolbachik fissure eruption 2012-2013. SO RAN Publishing House,
542 Novosibirsk, p. 241-255 (in Russian).
543 Kazuchits, N.M., Rusetsky, M.S., Kazuchits, V.N., and Zaitsev, A.M. (2016) Aggregation of nitrogen in
544 synthetic diamonds annealed at high temperature without stabilizing pressure. Diamond and
545 Related Materials 64, 202–207. DOI: 10.1016/j.diamond.2016.03.002.
546 Klages, C.-P., and Schäfer, L. (1998) Hot-filament deposition of diamond. In: B. Dischler and C. Wild
547 (Eds.), Low-Pressure Synthetic Diamond. Springer-Verlag, Berlin, Heidelberg, pp. 85-94.
548 Khachtryan, G.K. (2013) Nitrogen and hydrogen in crystals of diamonds in the use of prognostication and
549 prospecting for diamond deposits. Otechestvennaya Geologia, No. 2, 29-40 (in Russian).
550 Kutyev, F.Sh., and Kutyeva, G.V. (1975) Diamonds in basaltoids of Kamchatka. Doklady Akademii
551 Nauk SSSR 221(1), 183-186 (in Russian).
552 Lang, A.R., Vincent, R., Burton, N.C., and Makepeace, A.P.W. (1995) Studies of small inclusions in
553 synthetic diamonds by optical microscopy, microradiography and transmission electron
554 microscopy. Journal of Applied Crystallography 28, 690-699.
555 Litasov, K., Voropaev, S., Sevastyanov, V., Kagi, H., Ohfuji, H., Ishibashi, H., and Galimov, E. (2017)
556 Cuboctahedral diamonds from volcanic rocks of Kamchatka: Contamination or growth in unusual
557 environments? Japan Geoscience Union Meeting 2018 Abstract SIT25-03.

Litasov, K. D., Kagi, H., Voropaev, S. A., Hirata, T., Ohfuji, H., Ishibashi, H., Makino, Y., Bekker, T. B., Sevastyanov, V. S., Afanasiev, and V. P., Pokhilenko, N. P. (2019) Comparison of enigmatic diamonds from the Tolbachik arc volcano (Kamchatka) and Tibetan ophiolites: Assessing the role of contamination by synthetic materials. Gondwana Research 75, 16-27. DOI: 10.1016/j.gr.2019.04.007.

McCandless, T. E., Letendre, J., and Eastoe, C.J. (1999) Morphology and carbon isotope composition of microdiamonds from Dachine, French Guyana. In: J.J. Gurney, J.L. Gurney, M.D. Pascoe, S.H. Richardson (eds) Proceedings of the VIIth International Kimberlite Conference, vol. 2. Red Roof Design, Cape Town, 550-556.

McDonough, W.F., and Sun, S.-s. (1995) The composition of the Earth. Chemical Geology120 (3-4), 223-253.

McNamara, K.M. (2003) Aggregate nitrogen in synthetic diamond. Applied Physics Letters 83(7), 1325–1327. DOI:10.1063/1.1347012.

Orlov, Yu.L. (1987) Mineralogy of Diamond. John Wiley & Sons, NY, 235 pp.

Palyanov, Yu.N., Khokhryakov, A.F., Borzdov, Yu. M., Sokol, A.G., Gusev, V.A., Rylov, G.M., and Sobolev, N.V. (1997) Growth conditions and real structure of synthetic diamond crystals. Russian Geology and Geophysics 38(5), 920-945.

Orlov, Yu.L. (1987) Mineralogy of Diamond. John Wiley & Sons, NY, 235 pp.

Pekov, I.V., Anikin, L.P., Chukanov, N.V., Belakovskiy, D.I., Yapaskurt, V.O., Sidorov, E.G., Britvin, S.N., and Zubkova, N.V. (2016) Deltalumite, IMA 2016-027. CNMNC Newsletter No. 32, August 2016, p. 919; Mineralogical Magazine, 80, 915– 922.

Pujol-Solà, N., Proenza, J.A., Garcia-Casco, A., González-Jiménez, J.-M., Andreazini, A., Melgarejo, J.C., and Gervilla, F. (2018) An alternative scenario on the origin of ultra-high pressure (UHP) and super-Reduced (SuR) minerals in ophiolitic chromitites: A case study from the Mercedita deposit (Eastern Cuba). Minerals 2018, 8, 433. DOI: 10.3390/min8100433.

583 Schmidt, M.W., Gao, C., Golubkova, A., Rohrbach, A., and Connolly, J.A. (2014) Natural moissanite
584 (SiC)—A low temperature mineral formed from highly fractionated ultra-reducing COH-fluids.
585 Progress in Earth and Planetary Science 1, 27. DOI: 10.1186/s40645-014-0027-0.
586 Seliverstov, V.A. (2009) Thermobarophyllic mineral paragenesrs of diamondiferous alkaline ultramafic
587 volcanic complex in Eastern Kamchatka. Vestnik KRAUNZ Earth Sciences № 1(13), 10-30 (in
588 Russian).
589 Shechtman, D., Hutchison, J.L., Robins, L.H., Farabaugh, E.N., and Feldman, A. (1993) Growth defects
590 in diamond films. Journal of Materials Research 8(3), 473-479.
591 Shinohara, H. (2013) Volatile flux from subduction zone volcanoes: Insights from a detailed evaluation of
592 the fluxes from volcanoes in Japan. Journal of Volcanology and Geothermal Research 268, 46–63.
593 DOI: 10.1016/j.jvolgeores.2013.10.007.
594 Shiryaev, A.A., and Gaillard, F. (2014) Local redox buffering by carbon at low pressures and the
595 formation of moissanite – natural SiC. European Journal of Mineralogy 26, 53–59. DOI:
596 10.1127/0935-1221/2013/0025-2339.
597 Silaev, V.I., Karpov, G.A., Rakin, V.I., Anikin, L.P., Vasiliev, E.A., Filippov, V.N., and Petrovskiy, V.A.
598 (2015) Diamonds in the products of Tolbachik fissure eruption 2012-2013, Kamchatka. Vestnik
599 Permskogo Universiteta, Vipusk 1(26), 6-27 (in Russian).
600 Smith, E.M., Shirey, S.B., Nestola, F., Bullock, E.S., Wang, J., Richardson, S.H., and Wang, W. (2016)
601 Large gem diamonds from metallic liquid in Earth's deep mantle. Science 354 (6318), 1403-1405.
602 DOI: 10.1126/science.aal1303.
603 Taylor, W.R., Canil, D., and Milledge, H.J. (1996) Kinetics of Ib to IaA nitrogen aggregation in
604 diamonds. Geochimica et Cosmochimica Acta 60(23), 4725-4733.
605 Volynets, A.O., Melnikov, D.V., and Yakushev, A.I. (2013) First data on composition of the volcanic
606 rocks of the IVS 50th anniversary Fissure Tolbachik eruption (Kamchatka). Doklady Earth
607 Sciences 452(1), 953–957. DOI: 10.1134/S1028334X13090201.

Wilson, R.G. (1995) SIMS quantification in Si, GaAs, and diamond – an update. International Journal of Mass Spectrometry and Ion Processes 143(1), 43-49.

Wirth, R. (2004) Focused Ion Beam (FIB) A novel technology for advanced application of micro- and nanoanalysis in geosciences and applied mineralogy. European Journal of Mineralogy 16, 863-877.

Wirth, R. (2009) Focused Ion Beam (FIB) combined with SEM and TEM: Advanced analytical tools for studies of chemical composition, microstructure and crystal structure in geomaterials on a nanometre scale. Chemical Geology 261, 217-229.

Xu, X., Cartigny, P., Yang, J., Dilek, Y., Xiong, F., and Guo, G. (2017) Fourier transform infrared spectroscopy data and carbon isotope characteristics of the ophiolite-hosted diamonds from the Luobusa ophiolite, Tibet, and Ray-Iz ophiolite, Polar Urals. Lithosphere 10(1), 156-169. DOI: 10.1130/L625.1.

Zelenski, M., and Taran, Yu. (2011) Geochemistry of volcanic and hydrothermal gases of Mutnovsky volcano, Kamchatka: Evidence for mantle, slab and atmosphere contributions to fluids of a typical arc volcano. Bulletin of Volcanology 73(4), 373-394. DOI: 10.1007/s00445-011-0449-0.

Zelenski, M., Malik, N., and Taran, Yu. (2014) Emissions of trace elements during the 2012–2013 effusive eruption of Tolbachik volcano, Kamchatka: enrichment factors, partition coefficients and aerosol contribution. Journal of Volcanology and Geothermal Research 285, 136–149. DOI: 10.1016/j.jvolgeores.2014.08.007.

**TABLES**

This is a preprint, the final version is subject to change, of the American Mineralogist (MSA)
Cite as Authors (Year) Title. American Mineralogist, in press.
DOI: https://doi.org/10.2138/am-2020-7119

Table 1. Concentrations of elements in diamond #1 (at/cm$^3$, ppm), obtained with the use of mass spectrometer Cameca IMS-4f and calculated on the basis of the Relative sensitivity factors (Wilson 1995), in comparison with concentrations of the elements in gases from the Tolbachik volcano

| Ion | Diamond #1 | | | Volcanic gases from Tolbachik (Zelenski et al. 2014) | |
|---|---|---|---|---|---|
| | Concentration, at/cm$^3$ | Concentration, ppm | Normalized to mantle pyrolite after McDonough and Sun (1995) | Concentration, ppm | Normalized to mantle pyrolite after McDonough and Sun (1995) |
| $N^+$* | $4.7 \times 10^{19}$ | 304 | 152.0 | | |
| $F^-$ | $6.8 \times 10^{17}$ | 5.6 | 0.2240 | 4650 | 186.0 |
| $Na^+$ | $6 \times 10^{16}$ | 0.6 | 0.2247 | 224 | 83.9 |
| $Al^+$ | $2.4 \times 10^{17}$ | 3 | 0.0001 | 7.9 | 0.0003 |
| $Si^+$ | $1.7 \times 10^{20}$ | 2200 | 0.0105 | 74 | 0.0004 |
| $Si^-$ | $2.4 \times 10^{16}$ | 310 | | | |
| $S^-$ | $7.7 \times 10^{17}$ | 11 | 0.0440 | 36000 | 144.0 |
| $Cl^-$ | $9.3 \times 10^{17}$ | 14.6 | 0,8588 | 24000 | 1411.8 |
| $K^+$ | $5.7 \times 10^{16}$ | 1 | 0.0042 | 250 | 1.0417 |
| $Ca^+$ | $1.8 \times 10^{17}$ | 3.3 | 0.0001 | 4.5 | 0.0002 |
| $O^-$ | $1 \times 10^{21}$ | 7382 | | | |

628
629

630

Table 2. Concentrations of nitrogen in the studied Tolbachik diamonds

| Sample # | Nitrogen (at. ppm) |
|---|---|
| T2 | 433 |
| T3 | 131 |
| TOP | 126 |
| CH | 245 |
| Average | 233.8 ± 143.8 (2s) |

631

632

This is a preprint, the final version is subject to change, of the American Mineralogist (MSA)
Cite as Authors (Year) Title. American Mineralogist, in press.
DOI: https://doi.org/10.2138/am-2020-7119

Table 3. Isotopic compositions of diamonds from the Tolbachik volcano

| Sample # | $\delta^{13}C_{VPDB}$, ‰ | $d^{15}N_{Air}$, ‰ | N, ppm |
|---|---|---|---|
| 2 | -26.73 | -2.58 | 97 ± 11 (2s) |
| 3 | -28.66 | -2.32 | 288 ± 16 (2s) |

633
634

635

Table 4. Chemical compositions of mineral inclusions in diamonds from the Tolbachik volcano (at.%)

| Grain No. | T1 centre | | | | T1 rim | | T2 centre | | T3 rim | |
|---|---|---|---|---|---|---|---|---|---|---|
| Inclusion No. | 1 | 1a | 2 | 3 | 1 | 2 | 1 | 1a | 1 | 1a |
| Si | 5.60 | 45.91 | 26.12 | 20.50 | - | 28.51 | 5.20 | 27.00 | 1.07 | 5.42 |
| Mn | 49.35 | 54.09 | 59.50 | 56.00 | 67.40 | 71.49 | 62.82 | 72.77 | 45.64 | 49.19 |
| Ni | 45.05 | - | 14.38 | 23.50 | 32.60 | - | 31.98 | 0.23 | 53.29 | 45.39 |
| Stoichiometry | MnNi | MnSi | $(Mn,Ni)_5Si_2$ | $(Mn,Ni)_4Si$ | $Mn_2Ni$ | $Mn_5Si_2$ | $Mn_2Ni$ | $Mn_5Si_2$ | MnNi | MnNi |

636
637

638

639

640 **CAPTIONS TO FIGURES**

641

642 Fig. 1. A map of the 2012-2013 Tolbachik lava flows. Yellow- lava fields; red line – the fissure; red stars
643 – diamond finds. The map is compiled with the use of space images by NASA and JPL and field works.
644 Details in the text.

645

646 Fig. 2. Eruption from the Naboko vent at the foot of the Plosky (Flat) Tolbachik volcano. Pyroclastic
647 material (black particles at the top of the volcanic material) formed a significant part of the eruption. 6
648 January 2013. Photo by A.A. Sokorenko.

649

650 Fig. 3. *In situ* microcrystal of diamond (shown with arrows) on the surface of deltalumite (a, b) and an
651 EDX spectrum of the diamond grain (c).
652
653 Fig. 4. Diamonds from the Tolbachik volcano.
654
655 Fig. 5. Details of the internal structure of diamonds from Tolbachik and mineral inclusions in them. A –
656 Typical homogeneous structure of diamond with no stacking faults, dislocations, cracks or low-angle
657 boundaries. Crystal T1-rim, foil #5576. B –Stacking faults and cracks in the central part of crystal T1, foil
658 #5575. C – Polymineral inclusion #1 of Mn-Ni alloy and Mn-silicide in crystal T1-centre, foil #5575.
659 Numbers in the figure correspond to the analyses numbers in Table 1. D –Nano-pore (shown with an
660 arrow) in the periphery of inclusion #3 in crystal T1-centre, foil #5575.A and B are TEM bright-field
661 images; C and D are high-angle annular dark-field (HAADF) images.
662
663 Fig. 6. Mn-Ni alloy particles on the surfaces of a diamond (A) and an ash particle (B). D – diamond.
664
665 Fig. 7. Ion distributions of impurity elements in Tolbachik diamond #1, obtained with the use of mass
666 spectrometer CamecaIMS-4f. Concentrations of elements (at/cm$^3$) are expressed in color. Areas out of
667 crystal boundary limits (dark blue) are metallic In, which the diamond crystal was mounted in.
668
669 Fig. 8. Mantle-normalized concentrations of elements in diamond #1 and in gas from the Tolbachik
670 volcano.
671
672 Fig. 9. FTIR spectrum of diamond #TOP.
673
674 Fig. 10. Histogram of $\delta^{13}C_{VPDB}$ distribution in diamonds from the Tolbachik volcano.
675

676 Fig. 11. Carbon-nitrogen isotopic compositions of diamonds from the Tolbachik volcano, on the
677 background of isotopic compositions of diamonds from different sources.
678
679 Fig. 12. Compositions of mineral inclusions in Tolbachik diamonds. Dotted lines indicate compositions of
680 inclusions in diamond crystallites from the Avacha volcano (Kaminsky et al. 2016). The compositional
681 fields of alloys (red) and silicides (blue) are outlined by solid lines. Fields, outlined by thin dotted lines,
682 are compositional fields of inclusions in polycrystalline diamond aggregates from the Avacha volcano
683 (Kaminsky et al. 2016). Details in the text.
684
685 Fig. 13. A – Mn-Ni alloy inclusion #1 in the rim of diamond T1, foil #5576. Note a pore shown with an
686 arrow. B - EDX spectrum from this inclusion. In addition to major element peaks (Mn and Ni), a strong C
687 peak is caused by the diamond host crystal. Minor admixtures of Cl, F and O are from the pores. The Cu-
688 $K_\alpha$ X-ray intensity is due to the copper grid on which the sample rests, and the Ga X-ray intensity
689 represents gallium implanted during the FIB sputtering.
690
691 Fig. 14. EDX spectra of the host diamond (B) and inclusions 2 and 3 (C and D) from the scanning
692 electron image (A).
693

Table 1. Concentrations of elements in diamond #1 (at/cm$^3$, ppm), obtained with the use of mass spectrometer Cameca IMS-4f and calculated on the basis of the Relative sensitivity factors (Wilson 1995), in comparison with concentrations of the elements in gases from the Tolbachik volcano

| Ion | Diamond #1 | | | Volcanic gases from Tolbachik (Zelenski et al. 2014) | |
|---|---|---|---|---|---|
| | Concentration, at/cm$^3$ | Concentration, ppm | Normalized to mantle pyrolite after McDonough and Sun (1995) | Concentration, ppm | Normalized to mantle pyrolite after McDonough and Sun (1995) |
| $N^+$* | $4.7 \times 10^{19}$ | 304 | 152.0 | | |
| $F^-$ | $6.8 \times 10^{17}$ | 5.6 | 0.2240 | 4650 | 186.0 |
| $Na^+$ | $6 \times 10^{16}$ | 0.6 | 0.2247 | 224 | 83.9 |
| $Al^+$ | $2.4 \times 10^{17}$ | 3 | 0.0001 | 7.9 | 0.0003 |
| $Si^+$ | $1.7 \times 10^{20}$ | 2200 | 0.0105 | 74 | 0.0004 |
| $Si^-$ | $2.4 \times 10^{16}$ | 310 | | | |
| $S^-$ | $7.7 \times 10^{17}$ | 11 | 0.0440 | 36000 | 144.0 |
| $Cl^-$ | $9.3 \times 10^{17}$ | 14.6 | 0,8588 | 24000 | 1411.8 |
| $K^+$ | $5.7 \times 10^{16}$ | 1 | 0.0042 | 250 | 1.0417 |
| $Ca^+$ | $1.8 \times 10^{17}$ | 3.3 | 0.0001 | 4.5 | 0.0002 |
| $O^-$ | $1 \times 10^{21}$ | 7382 | | | |

Table 2. Concentrations of nitrogen in the studied Tolbachik diamonds

| Sample # | Nitrogen (at. ppm) |
|---|---|
| T2 | 433 |
| T3 | 131 |
| TOP | 126 |
| CH | 245 |
| Average | 233.8 ± 143.8 (2σ) |

Table 3. Isotopic compositions of diamonds from the Tolbachik volcano

| Sample # | $\delta^{13}C_{VPDB}$, ‰ | $\delta^{15}N_{Air}$, ‰ | N, ppm |
|---|---|---|---|
| 2 | -26.73 | -2.58 | 97 ± 11 (2σ) |
| 3 | -28.66 | -2.32 | 288 ± 16 (2σ) |

Table 4. Chemical compositions of mineral inclusions in diamonds from the Tolbachik volcano (at.%)

| Grain No. | T1 centre | | | | T1 rim | | T2 centre | | T3 rim | |
|---|---|---|---|---|---|---|---|---|---|---|
| Inclusion No. | 1 | 1a | 2 | 3 | 1 | 2 | 1 | 1a | 1 | 1a |
| Si | 5.60 | 45.91 | 26.12 | 20.50 | - | 28.51 | 5.20 | 27.00 | 1.07 | 5.42 |
| Mn | 49.35 | 54.09 | 59.50 | 56.00 | 67.40 | 71.49 | 62.82 | 72.77 | 45.64 | 49.19 |
| Ni | 45.05 | - | 14.38 | 23.50 | 32.60 | - | 31.98 | 0.23 | 53.29 | 45.39 |
| Stoichiometry | MnNi | MnSi | $(Mn,Ni)_5Si_2$ | $(Mn,Ni)_4Si$ | $Mn_2Ni$ | $Mn_5Si_2$ | $Mn_2Ni$ | $Mn_5Si_2$ | MnNi | MnNi |

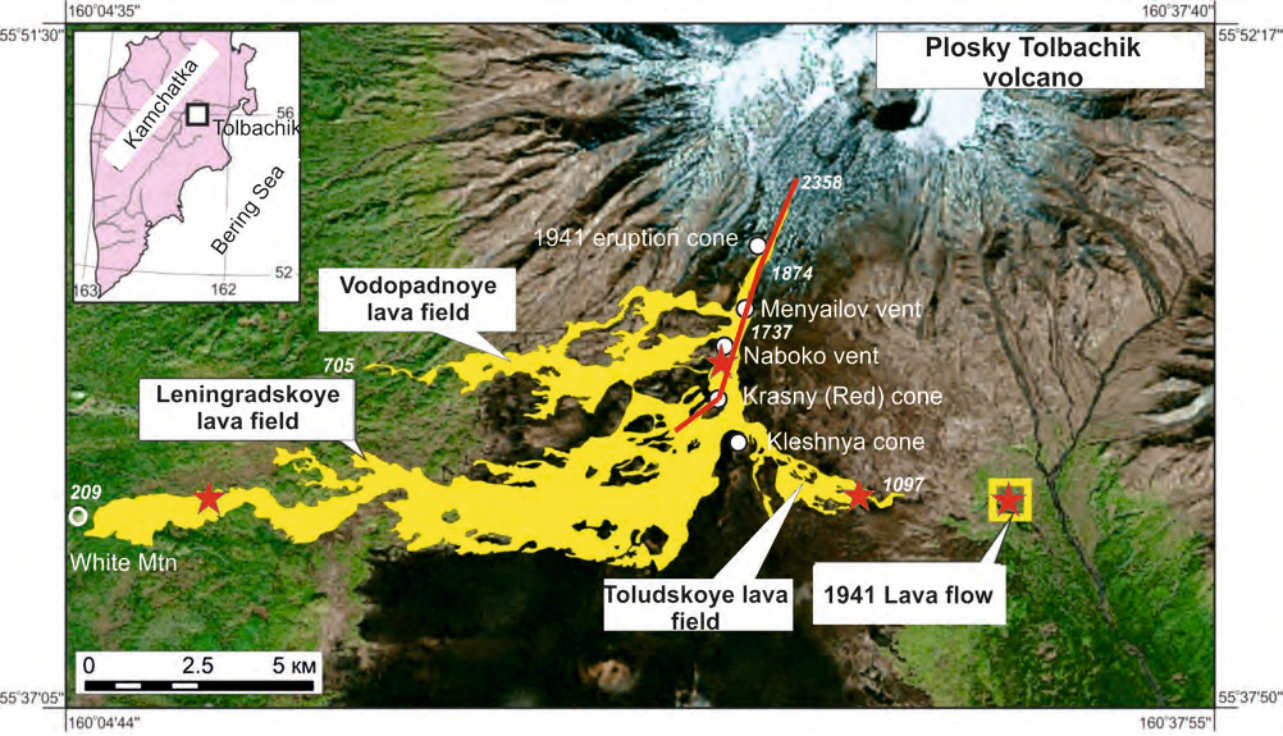
160°04'35"
160°37'40"
55°51'30"
55°52'17"
Plosky Tolbachik volcano
Kamchatka
Tolbachik
56
Bering Sea
52
163
162
2358
1941 eruption cone
1874
Vodopadnoye lava field
Menyailov vent
1737
Naboko vent
705
Leningradskoye lava field
Krasny (Red) cone
Kleshnya cone
209
1097
White Mtn
Toludskoye lava field
1941 Lava flow
0
2.5
5 км
55°37'05"
55°37'50"
160°04'44"
160°37'55"

Figure 1

Figure 2

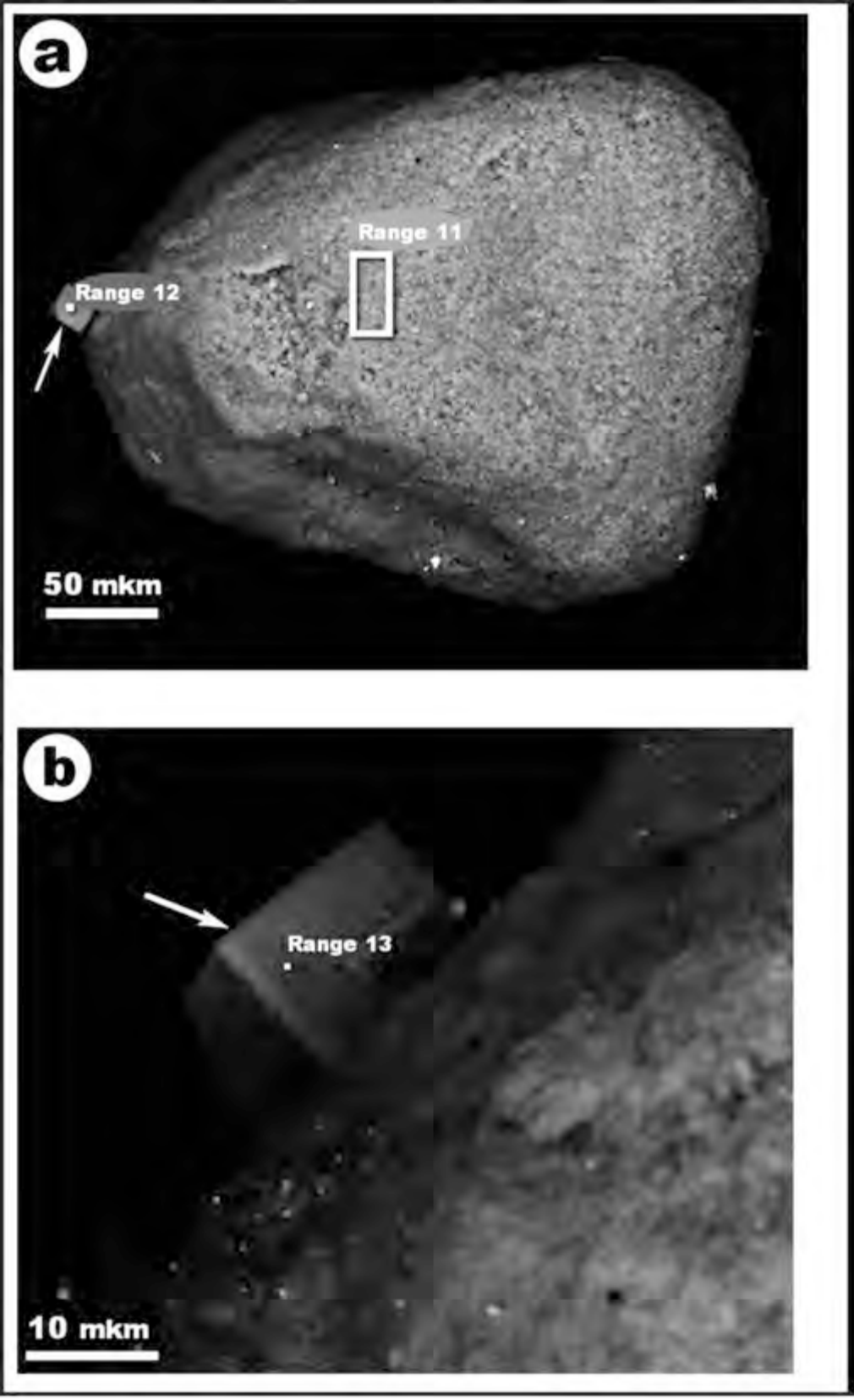
a
Range 11
Range 12
50 mkm
b
Range 13
10 mkm
c
Intensity
120
100
80
60
40
20
0
C
O
Na
Al
P
S
0
2
4
Energy, keV

Figure 3

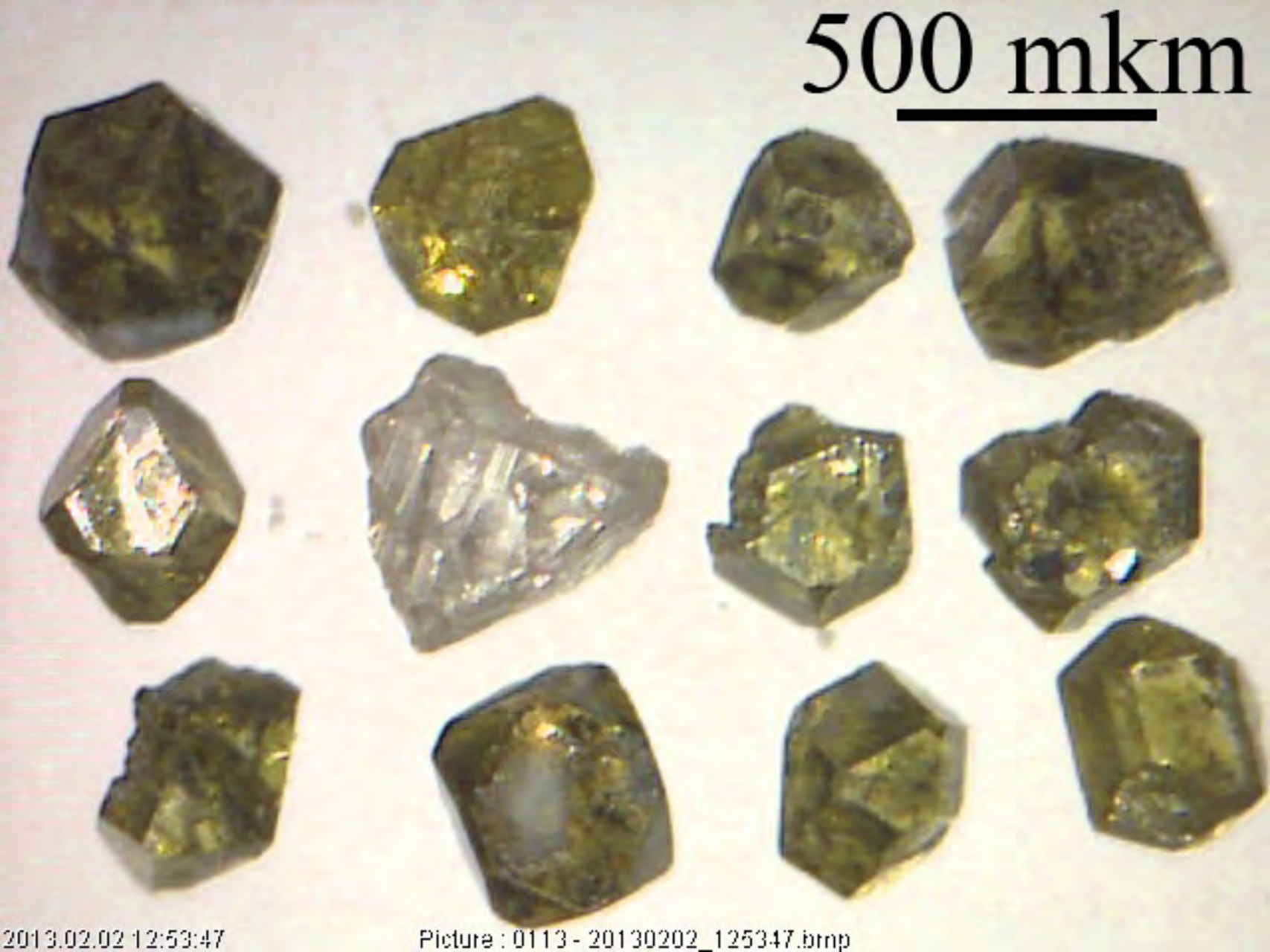
500 mkm
2013.02.02 12:53:47
Picture : 0113 - 20130202_125347.bmp

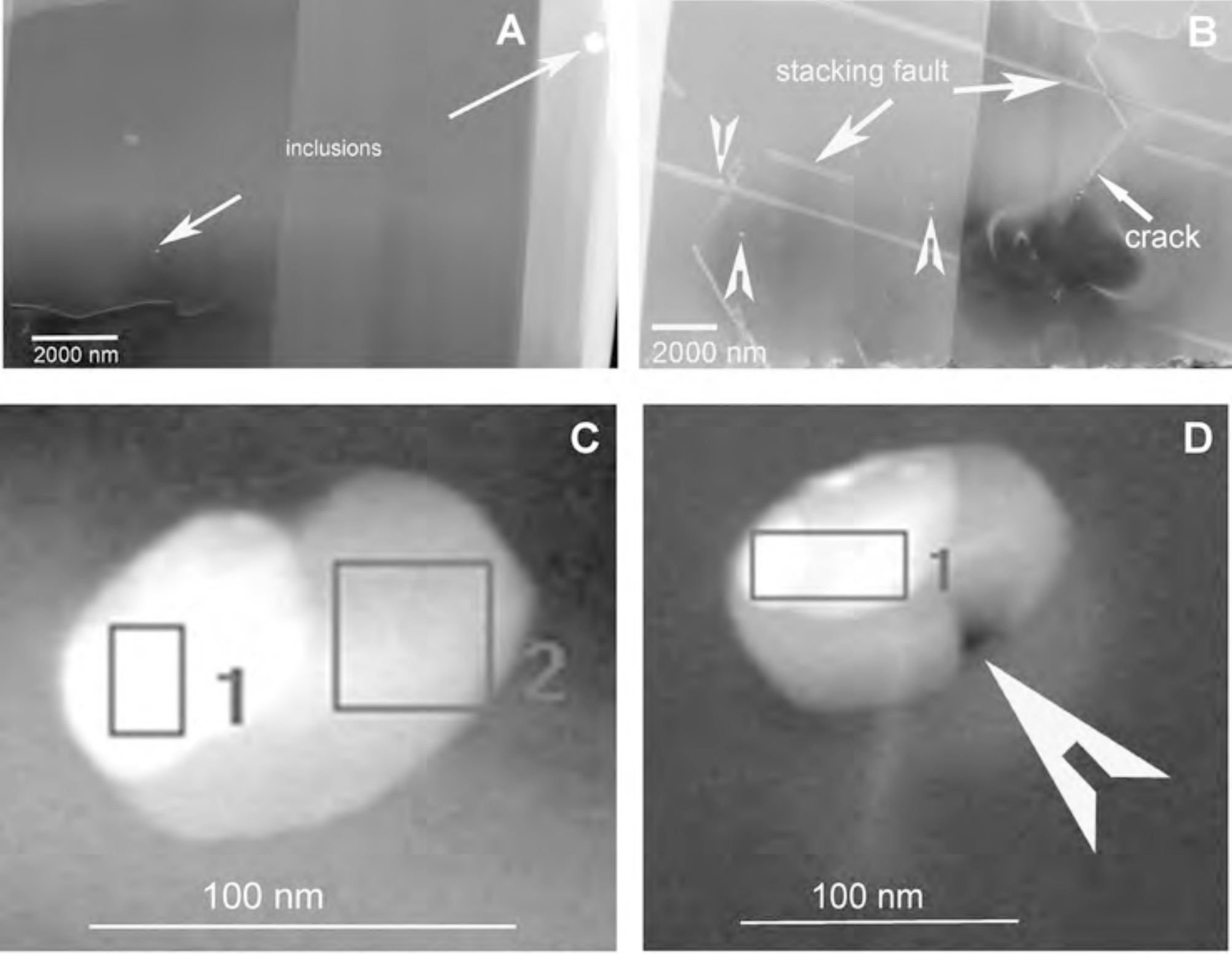
A
inclusions
2000 nm
B
stacking fault
crack
2000 nm
C
1
2
100 nm
D
1
100 nm

Figure 5

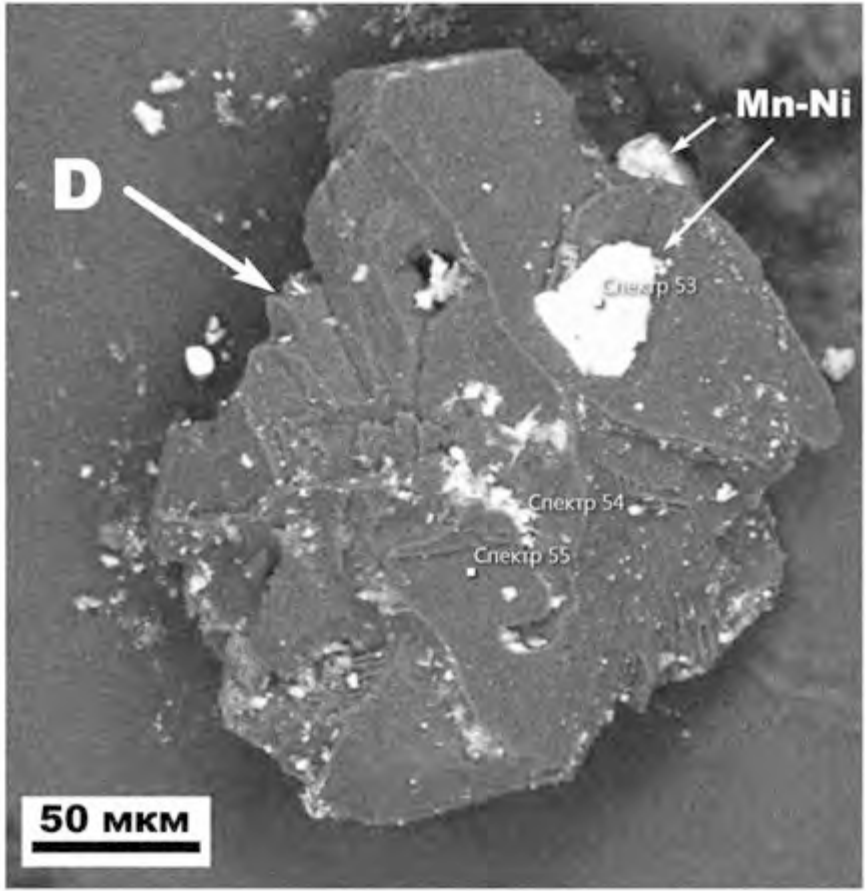
D
Mn-Ni
Спектр 53
Спектр 54
Спектр 55
50 мкм

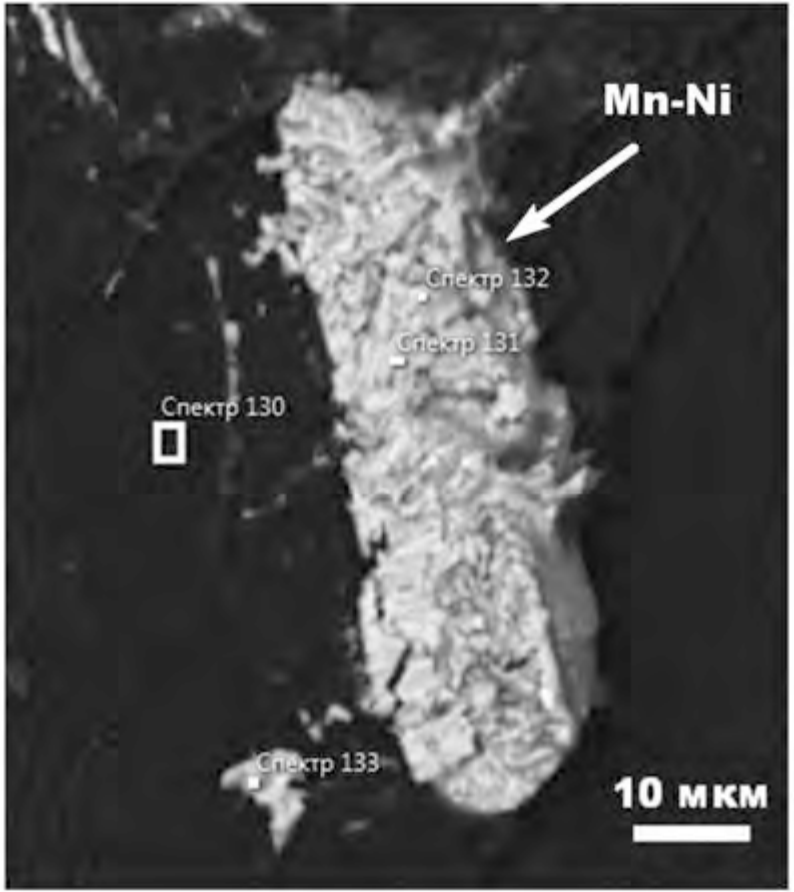
Mn-Ni
Спектр 132
Спектр 131
Спектр 130
Спектр 133
10 мкм

Figure 6

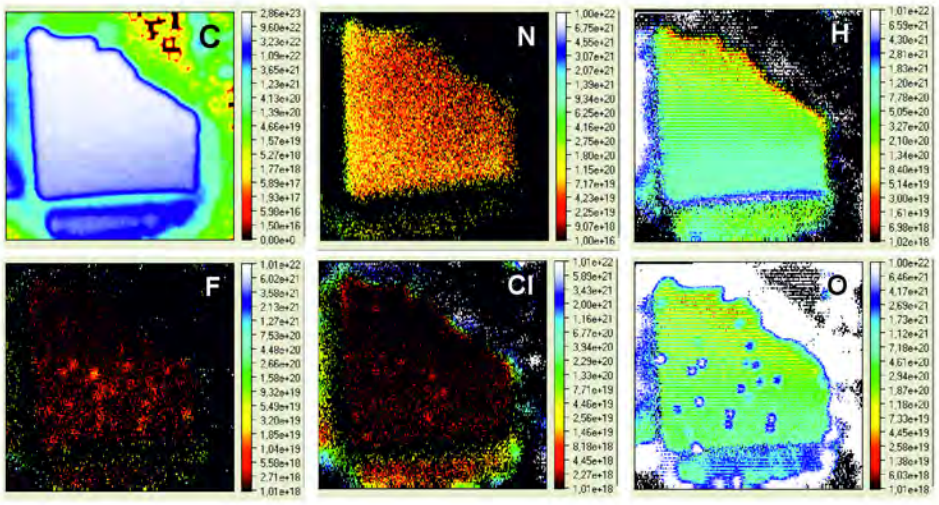
C
2.86e+23
9.60e+22
3.23e+22
1.09e+22
3.65e+21
1.23e+21
4.13e+20
1.39e+20
4.66e+19
1.57e+19
5.27e+18
1.77e+18
5.89e+17
1.93e+17
5.90e+16
1.50e+16
0.00e+0
N
1.00e+22
6.75e+21
4.55e+21
3.07e+21
2.07e+21
1.39e+21
9.34e+20
6.25e+20
4.16e+20
2.75e+20
1.80e+20
1.15e+20
7.17e+19
4.23e+19
2.25e+19
9.07e+18
1.00e+16
H
1.01e+22
6.59e+21
4.30e+21
2.81e+21
1.83e+21
1.20e+21
7.78e+20
5.05e+20
3.27e+20
2.10e+20
1.34e+20
8.40e+19
5.14e+19
3.00e+19
1.61e+19
6.98e+18
1.02e+18
F
1.01e+22
6.02e+21
3.58e+21
2.13e+21
1.27e+21
7.53e+20
4.48e+20
2.66e+20
1.58e+20
9.32e+19
5.49e+19
3.20e+19
1.85e+19
1.04e+19
5.58e+18
2.71e+18
1.01e+18
Cl
1.01e+22
5.83e+21
3.43e+21
2.00e+21
1.16e+21
6.77e+20
3.94e+20
2.29e+20
1.33e+20
7.71e+19
4.46e+19
2.56e+19
1.46e+19
8.18e+18
4.45e+18
2.27e+18
1.01e+18
O
1.00e+22
6.46e+21
4.17e+21
2.69e+21
1.73e+21
1.12e+21
7.18e+20
4.61e+20
2.94e+20
1.87e+20
1.18e+20
7.33e+19
4.45e+19
2.58e+19
1.38e+19
6.03e+18
1.01e+18

Figure 7

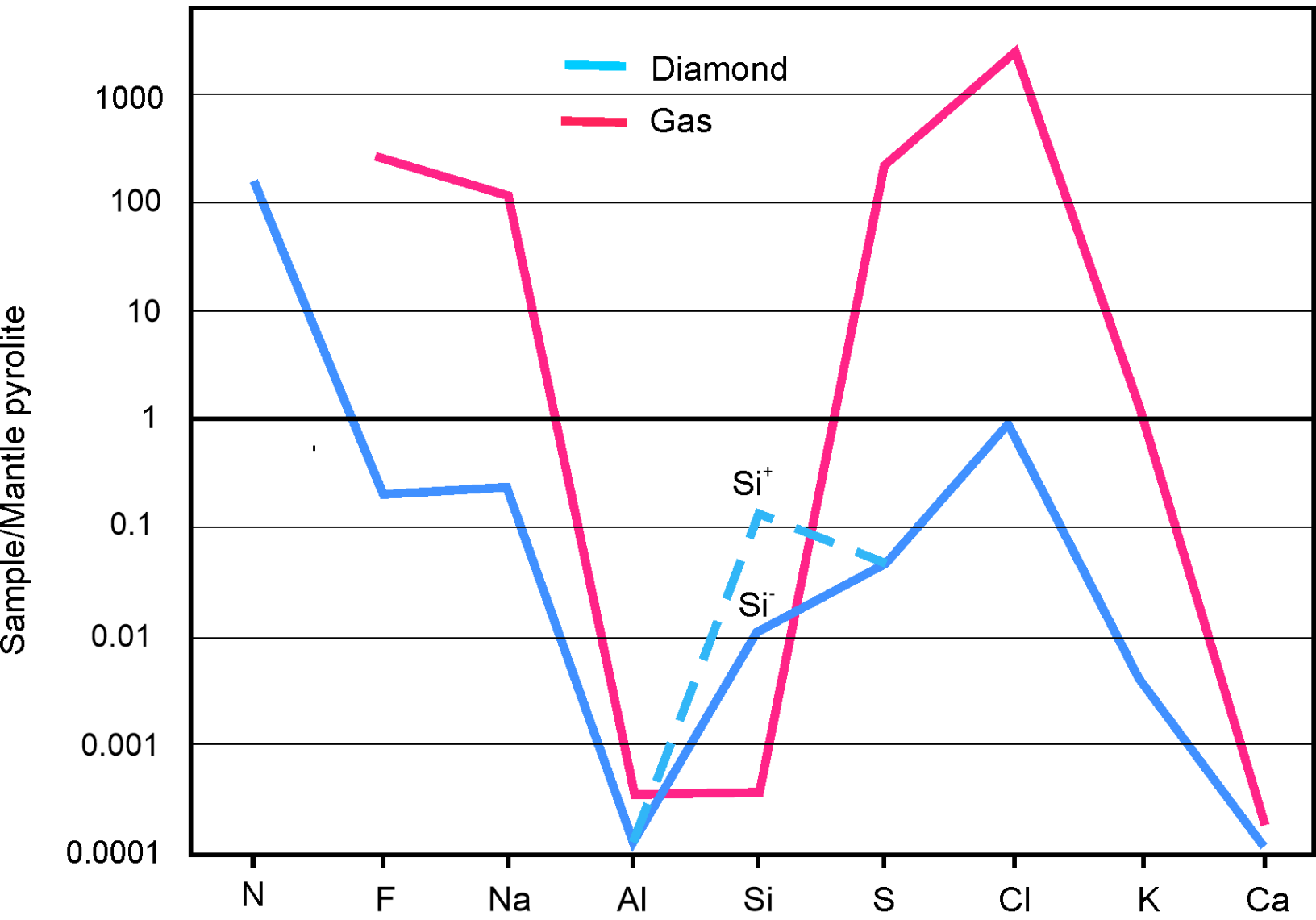
Diamond
Gas
1000
100
10
1
0.1
0.01
0.001
0.0001
Sample/Mantle pyrolite
Si+
Si-
N
F
Na
Al
Si
S
Cl
K
Ca

Figure 8

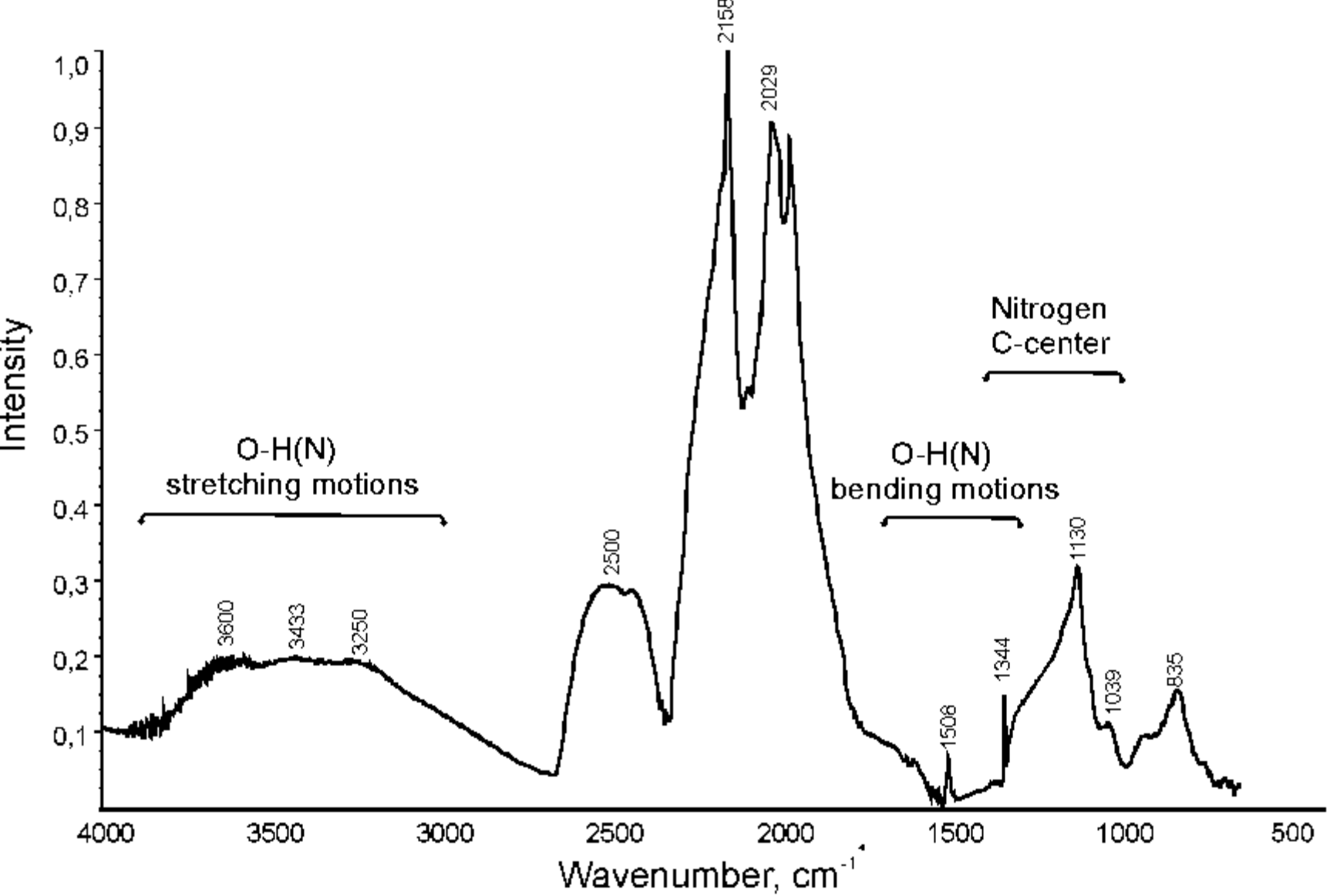
Intensity
1,0
0,9
0,8
0,7
0,6
0,5
0,4
0,3
0,2
0,1
O-H(N)
stretching motions
Nitrogen
C-center
O-H(N)
bending motions
3600
3433
3250
2500
2158
2029
1506
1344
1130
1039
835
4000
3500
3000
2500
2000
1500
1000
500
Wavenumber, cm-1

Figure 9

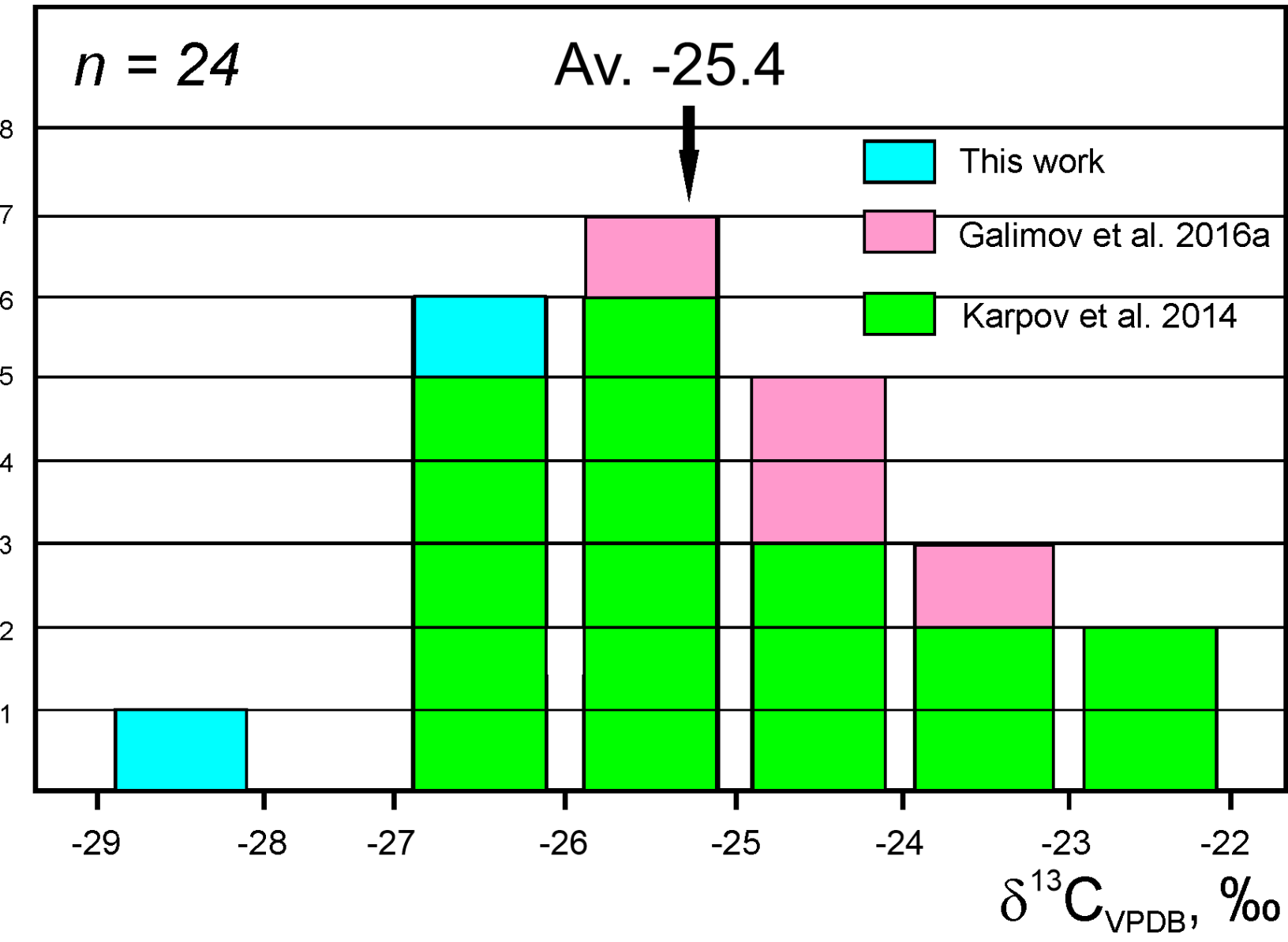
n = 24
Av. -25.4
This work
Galimov et al. 2016a
Karpov et al. 2014
8
7
6
5
4
3
2
1
-29
-28
-27
-26
-25
-24
-23
-22
δ13CVPDB, ‰

Figure 10

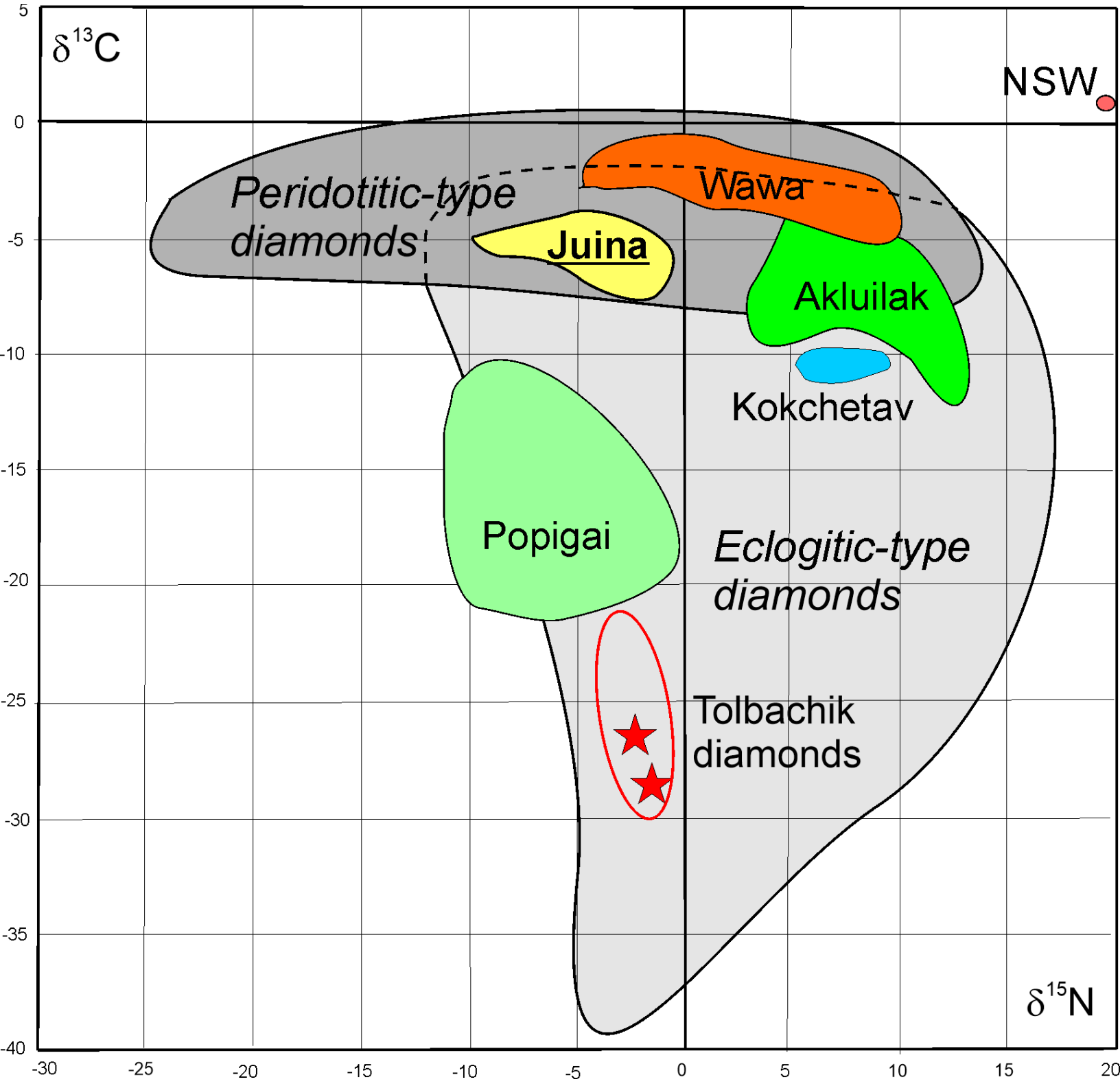
δ13C
NSW
Peridotitic-type diamonds
Wawa
Juina
Akluilak
Kokchetav
Popigai
Eclogitic-type diamonds
Tolbachik diamonds
δ15N
5
0
-5
-10
-15
-20
-25
-30
-35
-40
-30
-25
-20
-15
-10
-5
0
5
10
15
20

Figure 11

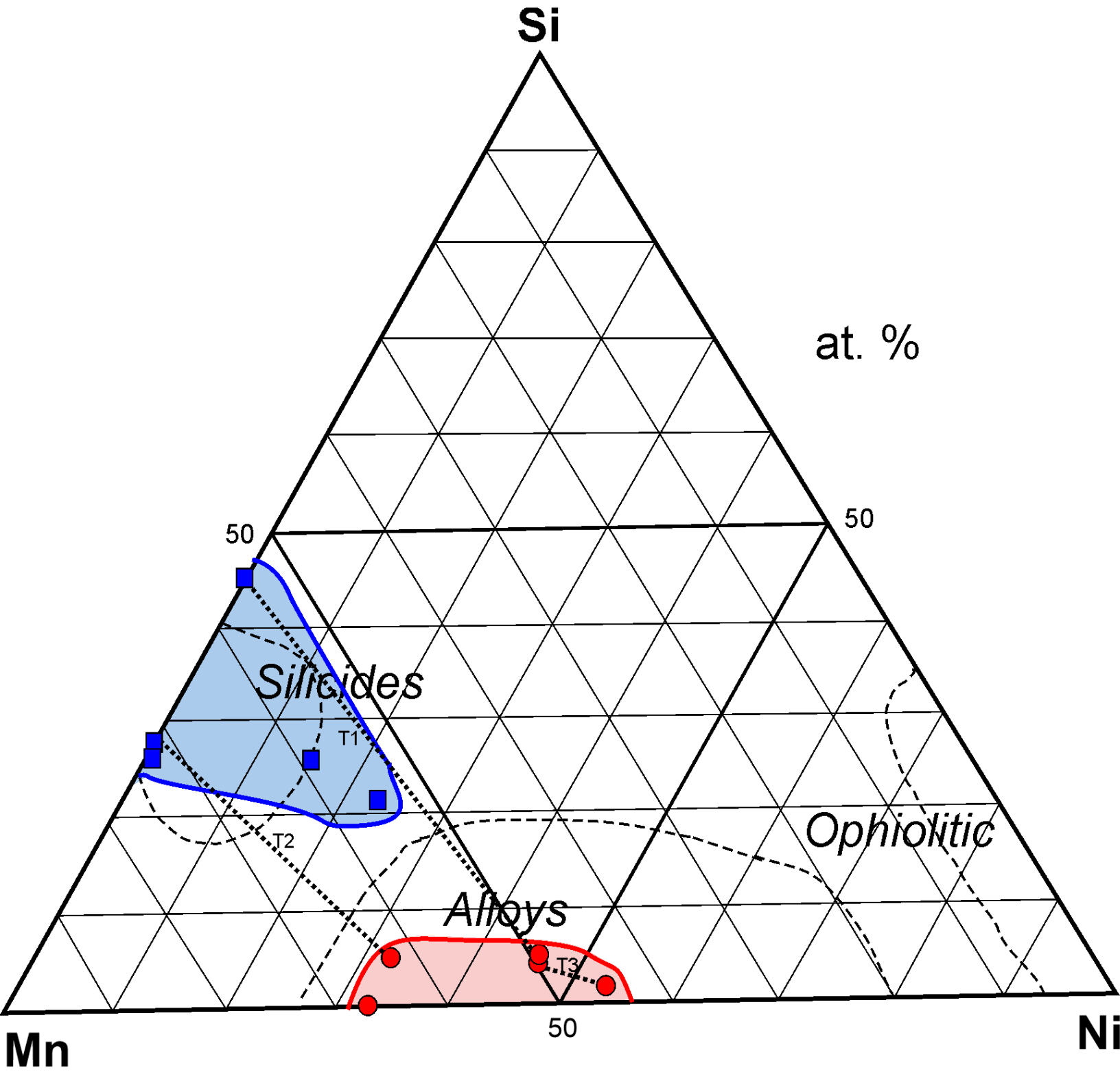


Figure 12

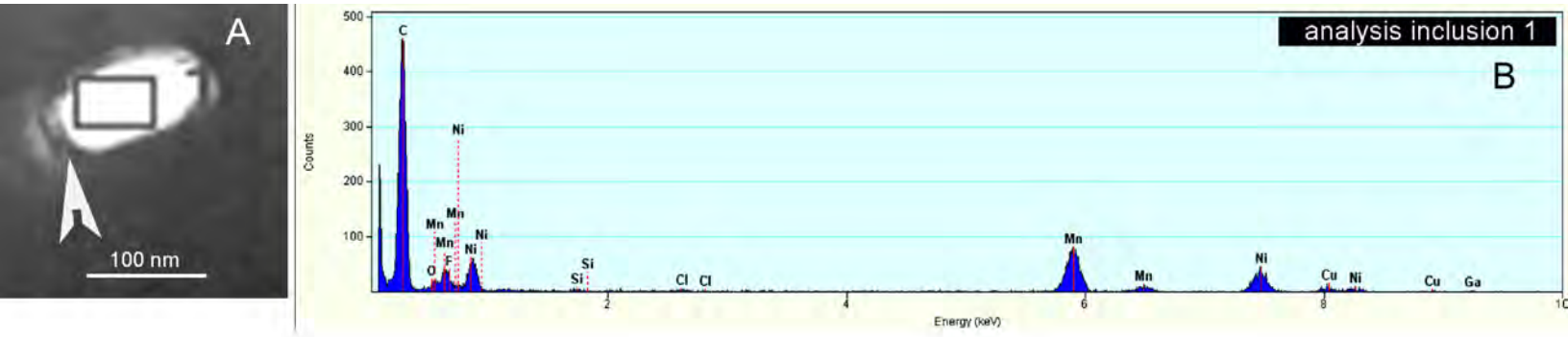
A
100 nm
analysis inclusion 1
B
Counts
Energy (keV)
C
Ni
Mn
Mn
Mn
Ni
Ni
O
F
Si
Si
Cl
Cl
Mn
Mn
Ni
Cu
Ni
Cu
Ga

Figure 13

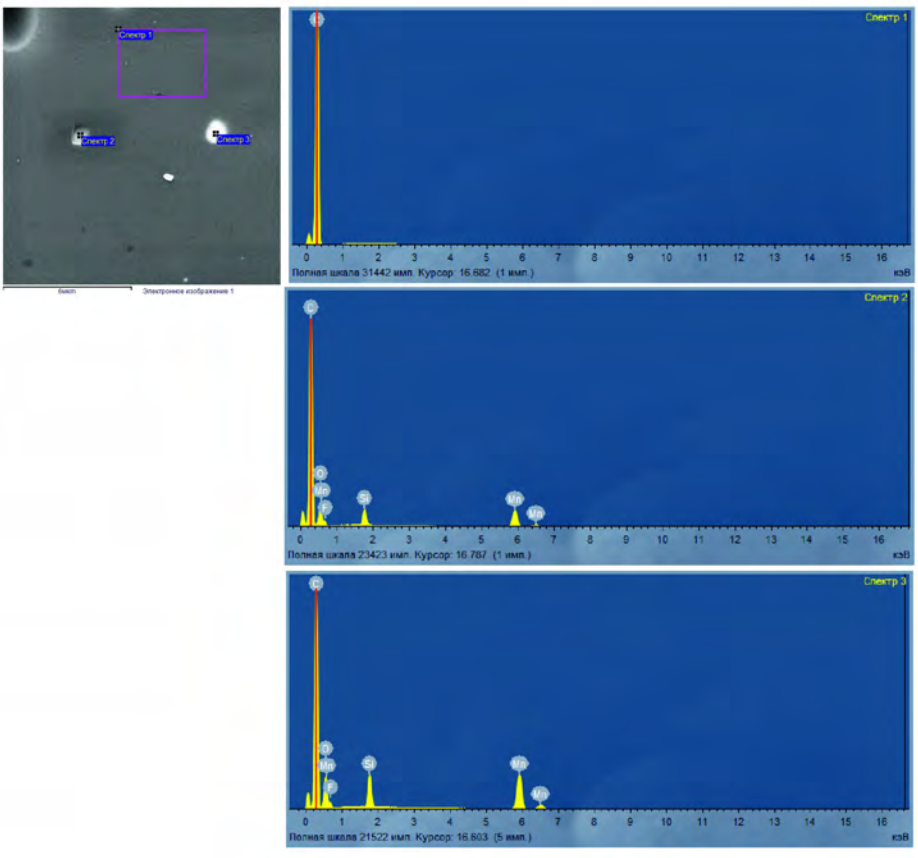
Спектр 1
Спектр 2
Спектр 3
Спектр 1
Полная шкала 31442 имп. Курсор: 16.682 (1 имп.)
кэВ
Спектр 2
Полная шкала 23423 имп. Курсор: 16.787 (1 имп.)
кэВ
Спектр 3
Полная шкала 21522 имп. Курсор: 16.803 (5 имп.)
кэВ

Figure 14.